University of Alberta

Wingless Localization Element 2 Functions Through Complex Formation

by

Nima Najand

A thesis submitted to the Faculty of Graduate Studies and Research
in partial fulfillment of the requirements for the degree of

Master of Science

Department of Cell Biology

Edmonton, Alberta
Fall 2007

Library and Archives Canada

Published Heritage Branch

395 Wellington Street
Ottawa ON K1A 0N4
Canada

Bibliothèque et Archives Canada

Direction du Patrimoine de l'édition

395, rue Wellington
Ottawa ON K1A 0N4
Canada

Your file Votre référence
ISBN: 978-0-494-33313-6
Our file Notre référence
ISBN: 978-0-494-33313-6

NOTICE:
The author has granted a non-exclusive license allowing Library and Archives Canada to reproduce, publish, archive, preserve, conserve, communicate to the public by telecommunication or on the Internet, loan, distribute and sell theses worldwide, for commercial or non-commercial purposes, in microform, paper, electronic and/or any other formats.

The author retains copyright ownership and moral rights in this thesis. Neither the thesis nor substantial extracts from it may be printed or otherwise reproduced without the author's permission.

AVIS:
L'auteur a accordé une licence non exclusive permettant à la Bibliothèque et Archives Canada de reproduire, publier, archiver, sauvegarder, conserver, transmettre au public par télécommunication ou par l'Internet, prêter, distribuer et vendre des thèses partout dans le monde, à des fins commerciales ou autres, sur support microforme, papier, électronique et/ou autres formats.

L'auteur conserve la propriété du droit d'auteur et des droits moraux qui protège cette thèse. Ni la thèse ni des extraits substantiels de celle-ci ne doivent être imprimés ou autrement reproduits sans son autorisation.

In compliance with the Canadian Privacy Act some supporting forms may have been removed from this thesis.

While these forms may be included in the document page count, their removal does not represent any loss of content from the thesis.

Conformément à la loi canadienne sur la protection de la vie privée, quelques formulaires secondaires ont été enlevés de cette thèse.

Bien que ces formulaires aient inclus dans la pagination, il n'y aura aucun contenu manquant.

Canada

In the arts, something seemingly simple is made exorbitantly complicated, while in the sciences, incredibly complex phenomena are reduced to an offensive simplicity.

Nima Najand

Dedication

This thesis is dedicated to the strongest woman I know – my mother.

Abstract

Apical localization of *wg* transcripts in polarized cells of *Drosophila* is believed to be important in the function of the gene. Previous data had identified three partially redundant localization elements within the *wg* 3' UTR (WLEs), each sufficient to localize *wg* mRNA. Here I show that the minimal WLE2 sequence is neither necessary nor sufficient to direct apical transport, and yet has the ability to influence WLE3 mediated RNA transport. Furthermore, when WLE2 and FL *wg* 3' UTR RNA sequences are injected simultaneously in trans, WLE2 is transported to the apical cortex of the syncytial blastoderm. We propose that co-transport of WLE2 is due to the formation of a complex through RNA-RNA or RNA-protein-RNA interactions with full length 3' UTR.

Acknowledgements

First and foremost, I wish to thank my supervisor Andrew Simmonds for providing me the opportunity to do this research. His continued support and constructive criticism taught me more in three years than my entire undergraduate career. I would also like to thank my committee members Paul Melançon and John Bell who helped me organize my thoughts, find holes in my research and write a cohesive thesis. My fellow lab members Julie Haskins, Mary Schneider, Hua Deng and Sarah Hughes made repeated failures more bearable, provided technical help through their expertise and many ideas. My friends from outside of my lab helped make my time more memorable. Their frequent visits, sympathy and endless entertainment made my experiences many fold more enjoyable. I would likely to specifically thank Gilberto dos Santos for his data on WLE3 and email exchanges that greatly aided my analysis of WLE2, Hua Deng, Ankush Garg, Monica Davis and Nadim Najand for their help in the creation of transgenic flies and the RTPCR protocol, Naomi Baker for the initial cloning of some of the WLE2-3 constructs, Honey Chan for her help with confocal microscopy and Rick Poirier for his help with DNA sequencing. None of this would have been possible without the support of my wife Sunita, whose unbounded love and dedication inspired me to achieve more than I ever thought I could, and encouraged me to continue when I no longer had the will. I am forever indebted to my siblings Neda, Nikoo and Nadim who influenced me since my childhood and helped make me who I am today, and my mother to whom I have dedicated this thesis.

Table of Contents

CHAPTER 1 - INTRODUCTION **1**

Polarization is important for cell function 2

RNA localization plays many important roles 2

Secreted Wg activates well characterized and conserved signalling pathways 4

The *wg* transport pathway is likely shared with other localized RNAs 4

***wg* localization requires sequences in the 3' UTR of the mRNA** 5

CHAPTER 2 - MATERIALS AND METHODS **10**

Gel Electrophoresis 11

Polymerase Chain Reaction (PCR) 11

DNA Sequencing 14

Immunoprecipitation and RT-PCR 14

RNA Probe Preparation 15

Alexa-Fluor labelled RNA for Direct Injections 18

Extraction of Total mRNA from Embryonic Lysates 18

Northern Immuno-Membrane Assay (NIMA) 18

Fluorescent *in situ* Hybridization (FISH) 19

Direct injection assay 20

LacZ tagged *wg* 3' UTR constructs 21

β-galactosidase ORF plasmid 22

Generation of transgenic stocks 23

Fly cultures 28

Software 28

CHAPTER 3 - RESULTS **29**

WLE2 is not sufficient for apical localization 30

WLE2 can affect WLE3 localization 34

WLE2 is involved in multimerization 43

CHAPTER 4 - DISCUSSION **47**

The necessity of RNA localization 48

The mechanisms of RNA localization 49

WLE2 does not act as a cis-acting localization signal 50

WLE2 influences WLE3 structure and function 56

WLE2 is able to form complexes with the *wg* 3' UTR 61

The validity of the direct injection assay 64

Future work 69

Summary 70

BIBLIOGRAPHY **72**

List of Tables

Table 2-1: List of primers used in sequencing and PCR reactions 12

Table 2-2: cDNAs used in the creation of anti-sense RNA probes 17

Table 2-3: A complete list of LacZ tagged WLE2-3 constructs and controls..... 24

Table 3-1: Mutations in WLE2 can influence the apical transport of the WLE2-3 constructs 37

Table 3-2: FISH results show that WLE2 can influence WLE3 mediated localization in the WLE2-3 construct 42

Table 4-1: The direct injection assay reflects the results obtained using FISH 67

List of Figures

Figure 1-1: Locations and structures of WLEs in the wg 3' UTR of Drosophila melanogaster 7

Figure 3-1: RNA transcribed from the minimal WLE2 sequence does not localize apically in the direct injection assay 31

Figure 3-2: WLE2 is not sufficient to localize a lacZ reporter sequence *in vivo* 33

Figure 3-3: Mutations in WLE2 and downstream regions tested for localization defects 35

Figure 3-4: Mutations in WLE2 can affect the apical transport of WLE2-3 injected into syncytial embryos 39

Figure 3-5: Mutations in WLE2 can affect the apical transport of the WLE2-3 construct *in vivo* 41

Figure 3-6: WLE2 can be co-transported by forming a complex with other localized RNAs 45

Figure 4-1: The secondary structure of WLE3 is affected by upstream and downstream sequences 53

Figure 4-2: Predicted structure of the wild-type WLE2-3 sequence 54

Figure 4-3: Magnified views of wild-type WLE2 and WLE3 in the WLE2-3 construct 55

Figure 4-4: The predicted structures of the wild-type WLE2-3 sequence compared to those of mutations LS11, Δ17, Δ7, Δ3 and Δ16 57

Figure 4-5: The predicted structures of the LS11 and Δ7 mutations 58

Figure 4-6: The predicted structures of the Δ17 and Δ3 mutations 60

List of Abbreviations

bcd – *bicoid* mRNA or gene

cDNA – Complementary DNA

DNA – Deoxyribonucleic acid

DTT – Dithiothreitol

en – *engrailed* mRNA or gene

evi – *evenness interrupted* gene

FISH – Fluorescent *in situ* hybridization

FL – Full length

fwd – Forward

GFP – Green fluorescent protein

grk – *gurken* gene

GSK3 – Glycogen synthase kinase-3

gw – *gawky* gene

h – *hairy* mRNA or gene

hb – *hunchback* mRNA or gene

hnRNP – Heterogeneous-nuclear ribonucleoproteins

LacZ – β-galactosidase

LRP – Low density lipoprotein-receptor related protein

LS – Linker scanner
MBP – myelin basic protein

MGA – Malachite Green aptamer

mRNA – Messenger ribonucleic acid

NIMA – Northern Immuno-Membrane Assay

nos – *nanos* mRNA or gene

NTP – Nucleotide tri-phosphate

osk – *oskar* mRNA or gene

PCR – Polymerase chain reaction

ptc – *patched* gene

rev – Reverse

RNA – Ribonucleic acid

RNP - Ribonucleoprotein

RTPCR – Reverse transcriptase polymerase chain reaction

UAS – Upstream activating sequence

UTR – Untranslated region

wg – *wingless* mRNA or gene

Wg – *wingless* protein

WGA – Wheat germ agglutinin

WLE – *wingless* localization element

wls – *wntless* gene

WNT – The collective name for the orthologs and paralogs of *wingless*

Wnt – *wntless* protein

ZBP – Zipcode-binding protein

Chapter 1
Introduction

Polarization is important for cell function

Polarization plays in important role in the function of many cells. The ability to unevenly distribute cytoplasmic and/or membranous constituents of a cell is a feature common to nearly all forms of life, ranging from monocellular prokaryotes to vertebrates. In prokaryotes, asymmetrical positioning of flagella is critical for the directional movement of motile bacteria (Shapiro et al., 2002). Asymmetry is also essential for the function of many different cell types in multicellular organisms. In epithelial cells lining the luminal walls of vertebrate intestines, the correct positioning of various pumps and channels on the apical and basal cellular membrane is necessary for the transport of nutrients from food into the bloodstream. Non-uniform distribution of cellular components also plays a key role in the development of multicellular organisms. The segregation of cytoplasmic components to different regions of the embryo in *Caenorhabditis elegans* leads to the creation of unequal daughter cells upon division. This, in turn, leads to differential gene expression patterns in the daughter cells and allows them to proceed through different differentiation pathways (Sulston et al., 1983). In syncytial embryos, such as those of *Drosophila melanogaster*, individual nuclei alter their gene expression in response to the gradients of localized morphogenic transcription factors. The localization of these transcription factors conveys both spatial and temporal information to the nuclei, which in turn, alter their gene expression to differentiate into the proper cell type.

RNA localization plays many important roles

Cellular polarization is achieved by the selective segregation of proteins, lipids and RNAs to sub-domains within the cell. Localization of proteins is often dependent on selective trafficking of the protein to its destination based on signal sequences within the polypeptide itself. However, there are many cases where non-uniform protein distribution is due to an underlying non-uniform mRNA distribution. Once translated from these localized RNAs, the resulting protein can form a concentration gradient and exert its effects in a concentration dependent manner. One such example is the posterior morphogen *nanos* (*nos*), which prohibits the translation of maternal *hunchback* (*hb*) transcripts in the posterior of the embryo (Wharton and Struhl, 1991). Segregation of *nos*

transcripts to a small region in the posterior of the embryo results in a gradient of *NOS* protein upon translation (Wang and Lehmann, 1991).

RNA localization is also important for short lived or highly reactive proteins such myelin basic protein (MBP) in murine oligodendrocytes. MBP is a part of the myelin sheath that surrounds neuronal axons, but due to its nature, it binds very efficiently to any cellular membrane that it may come into contact with. Because of this, transport of the protein to the ends of cellular processes without contacting any membranes is very difficult. To overcome this problem, the RNA encoding MBP is transported to the myelin compartment of the oligodendrocyte where it is translated locally (Colman et al., 1982; Trapp et al., 1987).

Yet another group of proteins that requires localized transcripts are those that are needed in high concentrations in specific cellular domains, or those where uniform expression would be detrimental. A classic example of this is β-actin mRNA in migrating chicken fibroblasts. β-actin mRNA is concentrated at the distal regions of lamellae where it polymerizes to form the actin network required for cell movement (Lawrence and Singer, 1986). mRNA localization prevents the actin from polymerizing during transport or polymerizing with γ-actin localized to the perinuclear region of the cell (Hill and Gunning, 1993). At the same time, this is more efficient, since a single transcript, once transported, can be translated many times (Warner et al., 1963).

There are also unknown reasons why localization of mRNA is important in the function of its corresponding protein. *wingless* (*wg*) mRNA has been shown to localize to the apical regions of *Drosophila* and other dipteran embryonic epithelial cells (Bullock et al., 2004; Simmonds et al., 2001; Wilkie and Davis, 2001), and this localization is necessary for the production of functional *wg* protein (Simmonds et al., 2001). The exact reasons for the necessity of *wg* transcript localization are unknown, but previous studies for apically localized pair-rule mRNAs speculate that peripheral invaginations of the syncytial blastoderm may prevent the lateral diffusion of the mRNAs and subsequent proteins, thereby allowing the genes to assert their influence in tight compartments within an otherwise syncytial blastoderm (Davis and Ish-Horowicz, 1991). Apical localization of *wg* mRNA is unlikely to be necessary for this reason, as uniformly distributed *wg* mRNA mimics a loss of function allele and not a gain of function allele as would be expected of

ectopic expression (Simmonds et al., 2001). Furthermore, *wg* is not expressed until three hours after fertilization, at which point cellularization has already occurred and the plasma membrane that now surrounds the nuclei would prevent the RNA from diffusing into neighbouring cells (Baker, 1988; Bejsovec and Martinez Arias, 1991).

Secreted Wg activates well characterized and conserved signalling pathways

Wg is a highly charged cysteine rich diffusible signalling protein necessary for defining the parasegmental boundary (Baker, 1987; Gonzalez et al., 1991). It was first discovered as a recessive mutation that leads to the conversion of the distal wing blade into notum (Sharma, 1973; Sharma and Chopra, 1976), and was later identified as a segment polarity gene required to establish regions of the larval cuticle devoid of denticles and define denticle identity (Baker, 1987; Nusslein-Volhard and Wieschaus, 1980). Independently, an ortholog of *wg* was found in mice as a retroviral insertion site (int-1) leading to mammary tumour genesis (Rijsewijk et al., 1987). As the genes were cloned, orthologs were also found in humans (van Ooyen et al., 1985), *Xenopus laevis* (Noordermeer et al., 1989) *Brachydanio rerio* (Molven et al., 1991) and nearly all metazoan phyla (Cadigan and Nusse, 1997). Collectively, the orthologs and paralogs of this gene are referred to as WNTs from the contraction of *wg* and *int-1*.

In the pathway referred to as the "canonical" pathway, secreted Wg acts through its receptor frizzled and its co-receptor, low density lipoprotein receptor-related protein (LRP), to deactivate the destruction complex, containing Axin and glycogen synthase kinase-3 (GSK3), responsible for ubiquitin mediated degradation of free cytoplasmic Armadillo. This stabilizes cytoplasmic Armadillo and allows it to enter the nucleus and interact with pangolin to induce the expression of downstream targets (Cox and Peifer, 1998; Wodarz and Nusse, 1998) including Engrailed (En) which activates transcription of the secreted protein hedgehog (Hh). Hh is taken up by the Wg expressing cells and maintains Wg expression through a positive feedback cycle (Ingham, 1993; Martizez Arias et al., 1988).Wg can also act in other pathways involved in planar cell polarity (Strutt, 2003).

The *wg* transport pathway is likely shared with other localized RNAs

While the Wg signalling pathway has been well studied and characterized, the reasons for and mechanisms of its transcript localization are less well understood. Once exported into the cytoplasm, *wg* transcripts are actively transported to the apical regions of the cell along microtubules via minus end directed dynein motors (Wilkie and Davis, 2001). Prior to *wg* expression, there are a number of apically localized transcripts in the embryonic blastoderm. Injection of fluorescently labelled *bicoid* (*bcd*) mRNA into these syncytial embryos results in apical transport of the injected RNA (Bullock and Ish-Horowicz, 2001), despite the fact that *bcd* mRNA is normally only present in the few hours of embryogenesis, after which it is degraded never expressed again until oogenesis in females (Surdej and Jacobs-Lorena, 1998). Furthermore, during the time the time *bcd* mRNA is present, it is localized to the anterior pole of the embryo (Berleth et al., 1988). Since *bcd* transcripts are able to be transported during times in development that they are not normally expressed suggests that the same machinery that is transporting other localized RNAs is also able to localize *bcd* if it is present. This also suggests that not only is there a common machinery, but that there are also shared sequences and motifs within localized RNAs that are recognized by the trans-acting factors. This point in further illustrated by the direct injection and *in situ* hybridization studies performed on *wg*. In the direct injection studies, *wg* RNA is injected into embryos prior to endogenous *wg* expression, yet the embryo is still able to transport the injected RNA apically, suggesting that the machinery required to transport *wg* mRNA is present before wild-type expression. Fluorescent *in situ* hybridization (FISH) studies show that *wg* mRNA foci co-localize with other apically localized mRNAs, likely because the same trans-acting factors are involved in the transport of multiple, different RNAs (Wilkie and Davis, 2001).

_wg_ localization requires sequences in the 3' UTR of the mRNA

Like many other localized transcripts such as *bcd* (MacDonald, 1990; Macdonald and Struhl, 1988), *osk* (Kim-Ha et al., 1993), *K10* (Cheung et al., 1992; Serano and Cohen, 1995), *nanos* (Gavis and Lehmann, 1992) and *hairy* (Bullock et al., 2003), the sequences required to direct the apical transport of *wg* mRNA have been mapped to discrete regions within the 3' UTR (Simmonds et al., 2001). Neither the open reading

frame nor the 5' UTR of *wg* transcripts is necessary or sufficient for the apical transport of the (Simmonds et al., 2001). It was believed that the 1098 nucleotide 3' UTR had two partially redundant regions responsible for *wg* mRNA localization. Initially, the *wg* localization elements (WLEs) were mapped to two ~100 nucleotide regions spanning nucleotides 55-181 for WLE1 and 672-771 for WLE2 (Figure 1-1). Each was shown to be sufficient to direct apical transport of either *wg* ORF mRNA or a *β-galactosidase* (LacZ) reporter gene fused 5' to them (Simmonds et al., 2001). Their localization activity was assessed by inducing the expression of a UAS-LacZ-WLE with a *patched*-Gal4 (*ptc*) driver in *Drosophila* embryos and performing FISH with a LacZ probe. The results showed that while each WLE had localization activity, neither mimicked the localization induced by the full 3' UTR exactly (Simmonds et al., 2001). Each WLE was then tested by direct injection into syncytial embryos. Preliminary results from these experiments showed that WLE1 did not localize in the direct injection assay while WLE2 had weak localization ability.

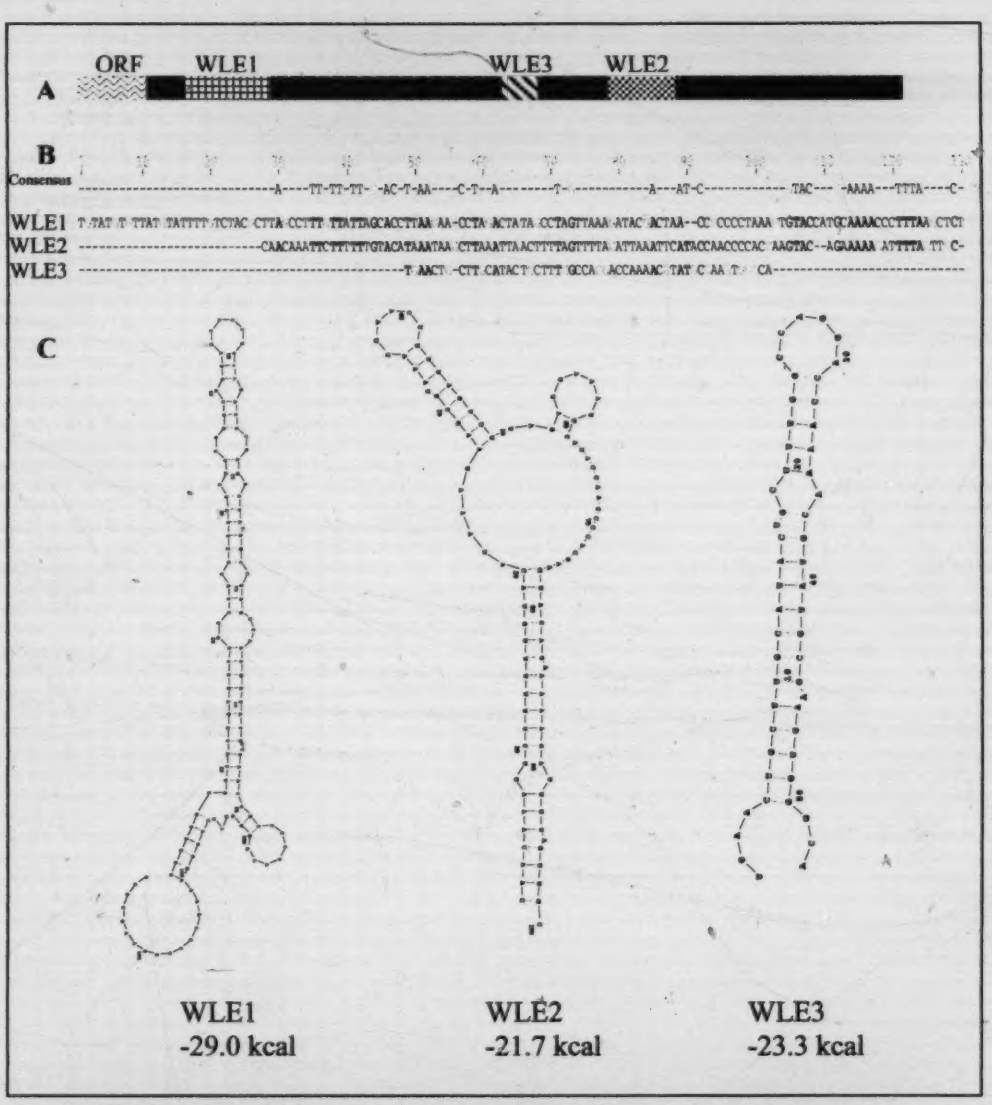

Figure 1-1: Locations and structures of WLEs in the *wg* 3' UTR of *Drosophila melanogaster*. **A)** A scaled schematic of the *wg* 3' UTR in *D. melanogaster* showing the relative locations of the three WLEs. The locations of WLE1 and WLE2 (Simmonds et al., 2001), and WLE3 (dos Santos, 2006). **B)** A sequence alignment of the three WLEs. The consensus derived from the alignment is based on nucleotides common to all three WLEs or two out of three if there is a gap in the third sequence. Coloured nucleotides represent bases that do not form a consensus. **C)** The predicted structures and enthalpies of the WLEs calculated using RNAstructure 4.4 at 25°C.

New data suggest that there is a third WLE located between WLE1 and WLE2 (518-570) (Figure 1-1). The function of this localization element has been studied using both FISH and the direct injection assay and has been shown to be sufficient to direct apical localization in both studies (dos Santos, 2006). Among the WLEs, apical localization mediated by WLE3 most closely resembles that of full length *wg* 3' UTR. These three WLEs have no apparent sequence or structural similarity to one another (Figure 1-1) or to the localization elements found in other RNAs, but do display some degree of evolutionary conservation (dos Santos, 2006). Phylogenetic analysis shows that WLE3 is most conserved, with 72% sequence identity and a well conserved predicted stem loop structure in the 20 *Drosophila* species analyzed (dos Santos, 2006). The first half of WLE1 (57-135) is also highly conserved, with a 77% sequence identity across all species examined (dos Santos, 2006). However, despite this high degree of conservation, the predicted structures for WLE1 from different species are quite different (dos Santos, 2006). WLE2 appears to be the least conserved, showing a sequence conservation no greater than the surrounding 3' UTR (dosSantos, 2006). Because of a general lack of selective pressure on UTRs due to their untranslated nature, conservation among these distantly related *Drosophila* species suggests some functional significance. Indeed, it has been shown that WLE3 from different *Drosophila* species retains its ability to direct apical localization when injected into *Drosophila melanogaster* embryos (dosSantos, 2006).

Given that these cis-acting sequencing are highly conserved between *Drosophila* species and appear to share machinery common to other localized RNAs, it is important to identify key nucleotides recognized by the trans-acting factors within the cell. In finding a consensus sequence necessary for the apical transport of this RNA, it is hoped that other localized RNAs can be identified through searches in the ever expanding genome databases. To accomplish this task, this thesis aims to address three major questions. 1) What is the exact function of WLE2? 2) What are the essential bases within WLE2? 3) Is the direct injection assay a valid method to analyze the localization of mRNA sequences?

This work establishes that the minimal WLE2 region is neither necessary nor sufficient for apical localization, and can only be localized in the presence of other *wg* 3' UTR sequences in trans. WLE2 influences the ability of WLE3 to localize, but its primary function is likely to dimerize with other parts of the *wg* 3' UTR either through direct RNA-RNA based interactions, or through protein mediated RNA-RNA interactions. RNA dimerization has been previously shown to promote localization of other mRNAs such as *bcd* (Ferrandon et al., 1997; Snee et al., 2005; Wagner et al., 2004), *hairy* (*h*) (Bullock et al., 2003) and *osk* (Hachet and Ephrussi, 2004). Intermolecular association of multiple strands of RNA might be a requisite for recognition by trans-acting factors, or it may be an evolutionary adaptation that allows multiple transcripts to be trafficked on one motor protein, thereby improving efficiency. It also has the potential to allow the transport of RNAs that are not directly recognized by adaptor proteins, but are transported indirectly by hitchhiking along with other RNAs. Indirect transport by binding other directly transported transcripts makes possible the localization of many different RNAs using fewer adaptor proteins. It also complicates the search for trans-acting factors as the proteins may not be directly binding to the RNA being tested.

In furthering our knowledge of WLE2 and its function, we hope to further our understanding of RNA localization and make generalization that hold true for other localized RNAs. If a consensus sequence required for dimerization or recognition by trans-acting factors is found, it will greatly aid the search for other localized RNAs as well as help unravel the RNA trafficking pathway.

Chapter 2
Materials and Methods

Gel Electrophoresis

Nucleic acid fragments were electrophoresed in standard gel loading buffer (2% glycerol v/v, 10mM Na_2EDTA pH 8.0, 0.1% w/v SDS, 0.0002% bromophenol blue w/v, 0.0002% w/v xylene cyanol) on a standard 0.8% to 2.0% w/v high purity agarose (Invitrogen) gel in TAE buffer (40mM Tris-acetate, 1mM EDTA pH 7.5) at 20V – 50V per 10cm of gel length. Ethidium bromide was added when the gel was cast, and nucleic acids were visualized on a UV light box or a gel imager. To resolve single stranded nucleic acids with considerable secondary structure, it was necessary to perform denaturing gel electrophoresis. This was done according to the Qiagen bench guide pages 57 -59 (2001). Alternatively, RNA was denatured at 65°C for five min in 75% de-ionized formamide and run on a standard agarose gel in TAE buffer (Masek et al., 2005).

Polymerase Chain Reaction (PCR)

PCR reactions typically consisted of 0.2 µM – 0.5 µM of each forward and reverse primer, 1.25 – 2 units of *Thermus aquaticus* or Platinum *pfx* polymerase (Invitrogen) per 50µl reaction, 1X of the supplied buffer, 1mM – 4mM (typically 1.5mM) $MgCl_2$, 10pg – 1µg of template DNA, 0.2mM dNTPs and de-ionized water to 50µl. The optimal conditions for each reaction were determined empirically. In situations where many similar PCR reactions were performed simultaneously, PCR supermix (Invitrogen) was used. Cycling conditions varied but were typically comprised of a 5 min denaturing step at 95°C, followed by 30 – 35 cycles of 1 min at 95°C, 30 sec – 1.5 min at 2°C - 5°C below the lowest annealing temperature of a primer set (for touchdown PCR reactions, the temperature was lowered 0.2°C – 0.5°C per cycle), and 1 min – 1.5 min at 75°C. These cycles were often followed by a 10 min elongation step at 75°C. For a list of primers used, see Table 2-1.

Table 2-1: List of primers used in sequencing and PCR reactions. primer sequences are always listed as 5' – 3' and melting temperatures calculated by supplier at 50mM Na^+. Where the supplier melting temperature was unavailable, it was calculated using pDraw. All non-starred primers are at a concentration of 100μM.

Name	Sequence	T_m (°C)	Uses	Comments
nanos cDNA fwd	GCAGACCAATGGCGGCAACTTAAT	60.1	Anneal to *nanos* RA cDNA	Pair will yield 1116bp from cDNA. Tested in RTPCR. Two ~correct bands
nanos cDNA rev	TAGCCGACGACGAAAGTGTTCCTT	60.0		
bicoid cDNA fwd	AGTTCGCGAGCGTCTCGAAAGTAA	60.0	Anneal to *bicoid* RA cDNA	Pair will yield 876bp from cDNA. RTPCR yields wrong sizes
bicoid cDNA rev	TAACTGGTTGCATATTCCCGGGCT	60.3		
Hsp83 cDNA fwd	ACAACGATGACGAGCAGTACGTGT	60.1	Anneal to Hsp83 RA cDNA	Pair will yield 789bp from cDNA. RTPCR yields correct band & incorrect ones
Hsp83 cDNA rev	TCTTCTTGACCAGGTTCTTGCGGA	60.0		
gurken cDNA fwd	TGGACAATCGGTCCACCCAATCAA	60.4	Anneal to *grk* RA cDNA	Pair will yield 703bp from cDNA. RTPCR yields correct size
gurken cDNA rev	TAACGCAGAGGCAGGAATGGAAGA	59.9		
odd skipped cDNA fwd	AGTTTGTGTCGAGACGTTGTCGGT	60.2	Anneal to *odd* RNA cDNA	Pair will yield 529bp from cDNA. Untested.
odd skipped cDNA rev	AAACTGGATACTGCTGTGGAGCCT	60.0		
even skipped cDNA fwd	AAGACGCATACCAAACATGCACGG	59.9	Anneal to *eve* RA cDNA	Pair will yield 406bp from cDNA. RTPCR yields correct band
even skipped cDNA rev	GATCCTCTGACGCTTGTCCTTCAT	58.3		
fushi tarazu cDNA fwd	GCAGAAGCTGAAGAATGGCGACTT	59.6	Anneal to *ftz* RA cDNA	Pair will yield 200bp from cDNA. RTPCR yields correct band
fushi tarazu cDNA rev	AAGTCTCCTCGATGTGCGACCAAT	60.0		
hairy cDNA fwd	AACAAGCCCATCATGGAGAAACGC	59.9	Anneal to *hairy* RB cDNA	Pair will yield 1078bp from cDNA. RTPCR yields correct band & incorrect ones.
hairy cDNA rev	CAAAGCAACATTTGCGCAATCCCG	59.9		
wingless cDNA fwd	AGTGTGTGTGCCGTCGAACAGATA	60.0	Anneal to *wg* RA cDNA	Pair will yield 700bp from cDNA. RTPCR has very low yield.
wingless cDNA rev	CGCCTCGTTGTTGTGCAGATTCAT	59.9		
engrailed cDNA fwd	TAACTGCTTCAATCCGGCTGCCTA	60.1	Anneal to *en* RB cDNA	Pair will yield 611bp from cDNA. RTPCR yields strong incorrect band.
engrailed cDNA rev	CGTTGGTCTTGTCCTTTGGCTGTT	59.7		
hedgehog cDNA fwd	ATGGATAACCACAGCTCAGTGCCT	60.0	Anneal to *hh* RB	Pair will yield 514bp from

hedgehog cDNA rev	AGTAGGCCAGCACGTTTAGCTTCT	60.0	cDNA	cDNA. RTPCR yields incorrect band.
Argonaute-1 cDNA fwd	AGAAAGCGGAAAGCGGATGAAAGC	60.0	Anneal to *ago1* RA cDNA	Pair will yield 264bp from cDNA. RTPCR yields correct band
Argonaute-1 cDNA rev	TCGCAAACTTGTGCCTGACATTCG	60.0		
Argonaute-2 cDNA fwd	TCACCATTGCGTCCTACTTCCACA	60.0	Anneal to *ago2* RB cDNA	Pair will yield 198bp from cDNA. RTPCR yields correct band
Argonaute-2 cDNA rev	TCGTCGATGTGGCTGCGTACTTTA	60.0		
β-tubulin 56D cDNA fwd	TGGGAACCCTGCTGATTTCCAAGA	60.3	Anneal to *β-tub* 56D RC cDNA	Pair will yield 564bp from cDNA. RTPCR yields strong correct band.
β-tubulin 56D cDNA rev	TCTGGATGTTCAGCATCTGCTCGT	60.0		
inscuteable cDNA fwd	ACAATCCGATAAGCAGCAAACGCC	60.0	Anneal to *insc* RA cDNA	Pair will yield 420bp from cDNA. No yield from RTPCR.
inscuteable cDNA rev	ACAGTTTCATTGTTGTACGGCGGC	60.1		
MGA sense	TCGAGGGGGGATCCCGACTGGCGAG AGCCAGGTAACGAATGGATCCCCCC	93	Seq. for malachite green aptamer	MGA aptamer + extra cloning sequences.
MGA anti-sense	TCGAGGGGGGATCCATTCGTTACCT GGCTCTCGCCAGTCGGGATCCCCCC	93		
MGA PCR fwd	GAGAGCCAGGTAACGAATG	56	Test orientation	Functional in PCR of MGA in pBSIISK
WLE1 fwd	GTATTTTGTCTACGCTTAGCC	54	PCR	Binds sense WLE1 sequence
pBSII rev	GCTTCCCGAAGGGAG	55	PCR	Anneals pBSII outside polylinker
mini-white rev	GCCTTCTAGTGGATCC	48	PCR screen	Screen MGA in pUAST-LacZ
pUAST 5' Seq	GCTAAGCGAAAGCTAAGC	53.8*	Sequencing primer	Obtained from AJS. Exact sequence uncertain
wg R7	CCAAGCAACTAAAATCTTTTTCTG	52.5*	PCR	Obtained from ASJ.
T3 fwd sequencing	ATTAACCCTCACTAAAGGGA	53.0	Sequencing	Binds to T3 RNA pol. promoter.
T7 fwd sequencing	TAATACGACTCACTATAGGG	47.0	Sequencing	Binds to T7 RNA pol. promoter.
gw exon 7 fwd	GGACGCAGTATTGGTGACGGTTGGC CTGATCCC	74.9*	PCR genotyping of *gw* mutation in *melano-gaster* embryos	Nested primers btained from Mary Schneider & AJS. Product of first set of nested primers not visible on agarose gel.
gw exon 8 rev	GGCAGTCAATCCTGGCGGGGGACCT CGAGACG	77.9*		
gw exon 7 fwd inside	TGGTCTGTTGCTCAGCCAACTTCA	65.2*		
gw exon 8 rev inside	TCCGAAGTGGCGGTACATTGTTGA	65.0*		

DNA Sequencing

Sequencing was done according to modified instructions for ABI Big Dye sequencing reactions (Applied Biosystems). A typical 20µl reaction consisted of 0.25µg of template DNA, 0.25µM primer, 3.0µl of ABI Terminator Ready Reaction Mix (Applied Biosystems), 0.625X of 5X Big Dye reaction buffer and de-ionized water. Cycling conditions typically included 2 min at 96°C, followed by 25 cycles of 46 sec at 96°C, 76 sec at 2°C - 5°C below the melting temperature of the primer and 4 min 10sec at 60°C. The reactions were precipitated with 65% isopropanol, incubated at room temperature for 30 min, centrifuged at maximum speed for 20 min, washed twice with 75% isopropanol and dried at 70°C for 20 min. For a list of primers used in sequencing reactions, refer to Table 2-1.

Immunoprecipitation and RT-PCR

To identify RNAs in complex with *gawky* (*gw*), UAS-Flag:HA:*gw* (Schneider et al., 2006) was expressed using a *nos*-Gal4 driver. The ribonucleoprotein complex was then immunoprecipitated using a protocol modified from Nelson et al. (2004). 0-3 hour embryos were collected and dechorionated in a 50% bleach solution. They were homogenized on ice in 5µl of lysis buffer (150mM KCl, 20mM Hepes-KOH pH 7.4, 1mM DTT and complete EDTA-free protease inhibitors (Roche)) to 1mg of embryos. Insoluble cellular debris were pelleted by centrifugation at 15000xg for 15 min at 4°C. The supernatant was collected and mixed with sterile glycerol to a final glycerol concentration of 10% v/v and frozen overnight at -80°C. Thawed lysates were diluted 1:1 with dilution buffer (100mM KCl, 30mM Hepes-KOH pH 7.4, 2% Tween-20 and protease inhibitors) and centrifuged at 15000xg for 15 min at 4°C. The supernatant was then collected, taking care not to draw from the lipid layer at the surface or the pellet at the bottom, and centrifuged as before. The supernatant was incubated with a 3:1000 dilution of rat anti-HA antibody on a rocker at room temperature for 30 min. Protein-G conjugated agarose beads were added to the solution at a concentration of 1:20 and incubated at 4°C for 2-3hours on a rocker. Beads were then washed 6 times with a 1:1 mixture of chilled lysis buffer and dilution buffer. 2µl of settled agarose beads were used in a subsequent RT-PCR reaction. A 20µl reverse transcriptase reaction consisted of

0.25μM reverse primer, 1X Superscript II reverse transcriptase buffer, 200 units of Superscript II reverse transcriptase (Invitrogen), 10mM DTT, 0.5mM dNTPs, 20 units of RNaseOUT (Invitrogen), 2μl of agarose beads from the previous immunoprecipitation and water. The immunoprecipated beads were first mixed with the primer and water and incubated at 70°C for 15 min then chilled on ice. The remaining components of the reverse transcriptase reaction were added to the chilled reaction and incubated at 45°C for 1 hour. The reaction was stopped with a 10 min incubation at 80°C. 3μl of the reverse transcriptase reaction was then used in a PCR reaction carried as described above.

RNA Probe Preparation

RNA probes used in FISH and Northern blots were hapten-labelled to allow recognition by antibodies. Digoxigenin (DIG) labelled RNA was created according to manufacturer's instructions (Roche) by linearizing the plasmid containing the desired sequences downstream of an RNA polymerase promoter with the appropriate restriction enzyme (Table 2-2). The plasmid was then purified by phenol/chloroform extractions. The transcription reaction was set up at room temperature to avoid the precipitation of the template by the spermadine in the RNA polymerase reaction buffer. A 20μl reaction contained 1μg- 2μg of template DNA, 2μl of DIG NTP labelling mix, 4μl of 5X transcription buffer of the corresponding RNA polymerase, 20 units of RNAseOUT (Invitrogen), 100 units of T7 or 30 units of SP6 or 40 units of T3 RNA polymerase and de-ionized water. The reaction was incubated at 37°C for 2 hours, then purified by LiCl precipitation (Hughes and Krause, 1999), or with Sephadex G-50 RNA spin columns according to manufacturer (Roche). RNA probes labelled with Alexa-Fluor 488 were transcribed as follows: 1μg - 2μg of linearized, phenol/chloroform purified template plasmid was added to a transcription reaction consisting of 2μl of NTP mix (5mM ATP, 5mM CTP, 5mM GTP and 3.25mM UTP), 3.5μl of 1mM Alexa-Fluor 488 conjugated UTP (Invitrogen), 0.6μl of 0.1M DTT, 20 units of RNaseOUT (Invitrogen), 4μl of 5X RNA polymerase buffer, 100 units of T7 or 30 units of SP6 or 40 units of T3 RNA polymerase and de-ionized water to 20μl. The reaction was assembled at room temperature and incubated at 37°C for 2 hours. Alexa-Fluor labelled RNAs were always purified using the Sephadex G-50 spin columns because ethanol precipitation appeared to

reduce the fluorescence and antigenicity of the fluorophore. It is important to note that when using RNA polymerase from New England Biolabs there was no detectable transcript produced, while RNA polymerases from Invitrogen or Fermentas consistently gave high yields. Although most protocols stress the importance of DTT in transcription reactions, my experience showed that when using RNA polymerase from Invitrogen, the addition of DTT was optional.

Table 2-2: cDNAs used in the creation of anti-sense RNA probes. RNA probes used in northern blots and FISH were transcribed from these plasmids. Comments include recommended restriction enzymes and RNA polymerases needed to transcribe anti-sense probes.

Gene Name	Clone ID	Vector	Resistance Marker	Comments
bicoid	LD36304	pOT2	Chloramphenicol	For anti-sense probes, digest with EcoRI & transcribe with SP6 RNA polymerase
Hsp83	AT20544	pOTB7	Chloramphenicol	For anti-sense probes, digest with BamHI & transcribe with T7 RNA polymerase
nanos	LD32741	pOT2	Chloramphenicol	For anti-sense probes, digest with EcoRI & transcribe with SP6 RNA polymerase
string	LD47579	pOT2	Chloramphenicol	For anti-sense probes, digest with EcoRV & transcribe with SP6 RNA polymerase
RpL32	RH03940	pFlc-1	Ampicillin	For anti-sense probes, digest with EcoRI & transcribe with T3 RNA polymerase
gawky	LD47780	pOT2	Chloramphenicol	For anti-sense probes, digest with EagI & transcribe with SP6 RNA polymerase
wingless	pAJS 1	pBS II SK-	Ampicillin	For anti-sense probes, digest with XbaI & transcribe with T7 RNA polymerase. Plasmid contains ORF only.
LacZ ORF	LacZ T7	pBS II SK+	Ampicillin	For anti-sense probes, digest with EcoRI & transcribe with T7 RNA polymerase. Plasmid contains ORF only.
LacZ ORF	LacZ T3	pBS II KS-	Ampicillin	For anti-sense probes, digest with EcoRI & transcribe with T3 RNA polymerase

Alexa-Fluor labelled RNA for Direct Injections

RNAs used in the direct injection assays did not require the same degree of fluorophore incorporation as those used as probes in the *in situ* hybridization. These transcription reactions consisted of 0.5µg – 2µg of linearized, phenol/chloroform extracted template DNA, 5µl of 5X RNA polymerase buffer, 1µl of NTP mix (10mM ATP, CTP, 3mM GTP), 1µl of UTP mix (0.9mM Alexa-Fluor labelled UTP (Invitrogen) and 9mM UTP), 2.5µl of 3mM 7meG cap analogue (Ambion), 0.75µl of 0.1mM DTT, 100 units of T7 or 30 units of SP6 or 40 units of T3 RNA polymerase (Invitrogen), 20 units of RNaseOUT, de-ionized water to 25µl. The reaction was incubated at 37°C for 2 hours, and purified using Sephadex G-50 spin columns (Roche).

Extraction of Total mRNA from Embryonic Lysates

RNAs from *Drosophila* lysates were obtained by Trizol extractions. Appropriately aged embryos were dechorionated in a 50% bleach solution and transferred into a 1.5ml microcentrifuge tube. Embryos were homogenized with a pestle in 500µl of Trizol (Invitrogen). Once all of the tissue had been homogenized, an additional 500µl of Trizol was added and the mixed solution was incubated at room temperature for 5 min. Insoluble debris were pelleted by centrifugation at 12000xg for 10 min at 4°C. The supernatant was transferred to a new tube and 200µl of chloroform was added and mixed by hand shaking. (Vortexing will shear genomic DNA and lead DNA contamination in the product). The solution was incubated for 3 min at room temperature and centrifuged at 12000xg for 15 min at 4°C. The colourless aqueous phase was transferred to a new tube and mixed with 500µl of isopropanol. The tube was incubated at room temperature for 10 min or longer periods at 4°C to increase yield. RNA was pelleted by centriguation at 16000xg for 15 min at 4°C. The supernatant was discarded and the pellet washed twice with 1ml of 75% ethanol with a 1 min maximum speed centrifugation at 4°C between washes. The pellet was briefly air dried and resuspended in nuclease free water or deionized water.

Northern Immuno-Membrane Assay (NIMA)

To non-radioactively detect very low concentrations RNA in various samples, an immunological detection method was employed. This technique was sensitive enough to detect the presence of *wg* RNA extracted from as few as 5 embryos. RNA samples were run on a denaturing gel as above and transferred onto a positively charged nylon membrane (Ambion) as described in the Qiagen bench guide page 57-66 (http://www1.qiagen.com/literature/BenchGuide/pdf/1017778_BenchGuide.pdf). The only modification of the protocol was the use of 10X instead of 20X SSC buffer as the transfer medium. After the transfer was completed, RNA was UV-crosslinked to the membrane with a 120mJ burst over 30sec. The blot was either used immediately or stored wet in 10X SSC at 4°C for short periods. The membrane was then pre-hybridized in 0.5ml/cm^2 of hybridization buffer (3M urea, 5X SSC, 0.1% w/v N-lauroylsarcosine, 0.02% w/v SDS, 0.5% BSA, 0.1mg/ml sonicated salmon sperm DNA) for 1 hour in a 68°C water bath in a sealed bag. DIG-labelled anti-sense RNA probe was added at concentration of 1:500 – 1:1000 and allowed to hybridize to targets overnight at 68°C. The membrane was then washed twice for 15 min each with 1ml/cm^2 of low stringency wash buffer (2X SSC, 0.1% SDS) and twice for 15 min each with high stringency wash buffer (0.1X SSC, 0.1% SDS) each pre-heated to 68°C. The wash buffer was removed and the membrane allowed to cool to room temperature. The membrane was incubated for 1 hour with 0.5ml/cm^2 of blocking buffer (0.1M maleic acid, 0.15M NaCl, 1.5% BSA, 0.1% Tween-20, pH 7.5) at room temperature. Blocking buffer was replaced with an equivalent volume of peroxidase conjugated sheep anti-DIG antibody (Roche) diluted to 1:10 000 in incubation buffer (0.1M maleic acid, 0.15M NaCl, 0.1% acetylated BSA, 0.1% Tween-20 pH 7.5) and placed on a rocker at room temperature for 15 min. Unbound antibody was removed with one 5 min and two 15 min washes with the blocking buffer. Chemiluminescent detection of the peroxidase conjugated antibody was then carried out according to the manufacture's directions (Pierce).

Fluorescent *in situ* Hybridization (FISH)

FISH was performed as described (Hughes and Krause, 1999) with the following variations. RNA probes were made as described above. Embryos were fixed by shaking them on a vortex equipped with a Styrofoam top carved to fit scintillation vials. It was found that the 20 min post fixation was not absolutely necessary although it did result in a

much higher proportion of stained embryos. When the embryos were post-fixed, they were fixed for 30 min instead of the recommended 20 min. Proteinase K digestion and the second post fixation step were found not to be necessary and somewhat detrimental to embryonic morphology. Double FISH was performed by using DIG and Alexa-Fluor 488 labelled RNA probes. The labelled RNAs were detected with sheep anti-DIG antibody at 1:2000 (Roche) and rabbit anti-Alexa488 antibody at 1:2000 (Invitrogen) respectively. Alexa-Fluor 555 conjugated donkey anti-sheep antibody at 1:4000 (Molecular Probes) and Alexa-Fluor 488 conjugated Donkey anti-rabbit 1:4000 (Molecular Probes) were used to detect the primary antibodies. Stained embryos were visualized using PerkinElmer spinning disc confocal microscope or LSM510 confocal microscope. Embryonic nuclei were counterstained with either the addition of 1:10 0000 dilution of 1mg/ml DAPI during the first wash of the secondary antibodies or 50ng/ml of Alexa-Fluor 647 conjugated wheat-germ agglutinin (Invitrogen) added at the same time as secondary antibodies. If nuclei were counterstained with DAPI, plasma membranes were stained with 1:2000 mouse anti-phosphotyrosine (Cell Signalling) primary antibody and 1:4000 Alexa-Fluor 647 donkey anti-mouse secondary (Molecular Probes). Single confocal slices were then analyzed to assess the proportion of RNA in each portion of the cell. Based on the position of the nucleus, the cell was divided into apical, middle and basal sections. Using ImageJ, the integrated density values of the RNA present in each section was measured and compared. For each construct tested, a minimum of three different embryos were measured to determine the average proportion of the RNA in the apical region of the cell. If greater than 45% of the RNA was in the apical region, it was classified as localized, if greater than 45% but less than 40% was in the apical region it was classified as partially locaized, and if less than 40% of the total RNA in the confocal slice was in the apical region, that construct was classified as unlocalized.

Direct injection assay

The direct injection assay was first described by Glozter et al. (1997) and later adapted and refined by Wilkie and Davis (2001). RNA to be injected was transcribed and labelled with Alexa-Fluor fluorophores as described above. Embryos expressing nuclear localization signal (NLS) tagged green fluorescent protein (GFP) (Davis et al., 1995) or

w^{1118} embryos were dechorionated in a 50% v/v bleach solution and rinsed with copious amounts of distilled water followed by a quick rinse with embryo wash (0.7% w/v NaCl, 0.04% Triton X-100 v/v) to detach embryos adhering to the walls of the collection chamber. Dechorionated embryos were then lined up end to end on a cover slip coated with a thin layer of embryo glue (1m of 3M double sided tape soaked in 50ml of heptane overnight). Embryos were then dehydrated in a sealed plastic container containing Drierite desiccant for 2-4 min depending on the relative humidity of the environment and the amount of time dechorionated embryos were exposed to ambient air. Dehydrated embryos on cover slips were then covered in a layer of halocarbon 700 oil (Halocarbon). The cover slip was attached with embryo glue to the center 3cm region cut out of a compact disc such that the halocarbon covered embryos are in the center region designed for the spindle and the cover slip is in contact with the region designed for the CD spindle platter. Additional halocarbon 700 oil was added to cover the entire spindle hole with oil. Embryos were aged to 2-3 hours at 25°C while in the assembled injection slide. To inject the embryos, the labelled RNA or mixture of RNAs was loaded into a needle, pulled from a glass capillary tube on a Flaming/Brown micropipette puller with microloader pipette tips (Eppendorf). To fill the needle tip and evacuate any bubbles present, the loading end of the needle was taped onto a microcentrifuge rotor and pulsed for <5sec at max acceleration with the lid open to prevent breakage of the tip. The needle was then used to radially inject the embryos while images were obtained on an Ultraview ERS spinning disc confocal microscope from PerkinElmer. The number of slices, slice thickness and exposure times varied between injections. Optimally, 10-15 slices were taken from the injection point to the bottom of the embryo with a 150-300ms exposure in each channel. In almost all cases, the images were taken on a Hamamatsu Orca AG camera binned 2x2 using a 20X plan-apochromat objective lens. All embryos were imaged for a minimum of 10 min or until no fluorescent RNA could be seen. Each RNA that appeared to localize was injected a minimum of four times, into four different embryos. Those RNAs that did not appear to localized were injected a minimum of ten times into different embryos, and if in all cases they still did not localize they were classified as non-localizing.

LacZ tagged *wg* 3' UTR constructs

Mutations along the wild-type WLE2-3 (355-1098) region of the *wg* 3' UTR were created using linker scanner mutagenesis to introduce *Bgl*II restriction sites and then cloned into a pSP72 vector. These plasmids were digested with *Cla*I and ligated into a double stranded *Spe*I linker oligonucleotide (CGACTAGTAT and CGATACTAGT). The mutated WLE2-3 regions were then excised from pSP72 with *Xba*I and *Spe*I and each was ligated to a pUAST-LacZ vector digested with *Xba*I. The presence and directionality of the insert was verified with a *Xba*I and *Xho*I double digestion. Positive clones were identified by the presence of a 773 nt band. Wild-type control WLE2-3 (355-1098) was derived from plasmid stock number pAJS 350. The 755 nucleotide region containing the full WLE2-3 region and some plasmid DNA was excised using *Bam*HI and *Bgl*II then gel purified. This was then ligated into pUAST-LacZ digested with *Bgl*II and screened for presence and directionality with a *Bgl*II and *Xba*I double digestion. LacZ tagged wild-type WLE2 (659-775) was derived from pAJS 131. After sequencing pAJS 131, it was found that this construct was in the opposite direction as to what was expected, however, when sub-cloned into pUAST-LacZ, the correct orientation was obtained and confirmed by sequencing. The WLE2 region was excised from pAJS 131 using *Bam*HI and ligated to a *Bgl*II digested pUAST-LacZ vector. The insert was screened by PCR with a pUAST 5' Seq forward primer and wgR7 reverse primer and sequenced with the pUAST-LacZ 3' sequencing primer (Table 2-1). Full length, wild-type control *wg* 3' UTR was obtained from a ~1kb *Bam*HI fragment and labelled as B1. This fragment was used to regenerate both pAJS 4 and pAJS 53 digesting pBSIISK+ with *Bam*HI and ligating the B1 fragment. Directionality of the insert was verified with a *Af*II and *Xba*I double digestion. The B1 fragment was also cloned into *Bgl*II digested pUAST-LacZ. The orientation of the fragment in this plasmid was checked with a *Afl*II and *Xba*I double digestion. The pUAST-LacZ vector was used as the negative control.

β-galactosidase ORF plasmid

In order to transcribe the LacZ ORF with the more efficient T7 RNA polymerase instead of T3, the direction of the ORF needed to be reversed. Because the LacZ insert was approximately the same size as the plasmid, excision of the insert in one step would have created two bands of approximately the same size, and this would make them difficult to

gel purify. To overcome this problem, the LacZ region was excised in two steps. First, the LacZ ORF was excised from the pBSIIKS+ plasmid by double digestion with *Eco*RI and *Sca*I. The resulting 4.4 kb fragment was gel purified and digested with *Hin*dIII yielding a 2.4 kb band that was purified and ligated to pBSIISK+ digested with *Eco*RI and *Hin*dIII. This plasmid was verified by single digestions with *Cla*I, *Eco*RI and *Pvu*II and sequenced with T7 forward and T3 forward sequencing primers (Table 2-1).

Generation of transgenic stocks

Genetic transformation of *Drosophila melanogaster* embryos was done through P-element mediated insertions (Rubin and Spradling, 1982). All transgenes were cloned into the p-UAST-LacZ vector containing flanking P-element insertion sites and microinjected into *y, w; Δ2-3, Sb/TM6, Ubx* embryos. In most cases, transgene insertions were mapped to a particular chromosome and the stocks maintained with floating balancers. In other instances, insertions were not mapped and stocks maintained either in a homozygous state or with the presence of balancers on chromosomes II and III. A list of transgenic stocks is included in Table 2-3.

Table 2-3: A complete list of LacZ tagged WLE2-3 constructs and controls. Fly strains that appear to have the same genotype differ due to the random P-element mediated insertion of the transgene. The linker scanner mutation numbers used throughout this thesis can be referenced to the original AJS DNA stock number from this table.

Stock Number	Genotype	Source	Comment
462	*w^{1118} P[w^+:UAS LacZ wg 3'UTR B1 1-1106]*	B1 Full *wg* 3' UTR	Tested by FISH, unmapped
239	*w^{1118} ; P[w^+:UAS LacZ wg 3'UTR 355-1098 pAJS 402]*	LS1 Transgene	Tested by FISH, mapped to chromosome II
240	*w^{1118}; ; P[w^+:UAS LacZ wg 3'UTR 355-1098 pAJS 402]*	LS1 Transgene	Tested by FISH, mapped to chromosome III
241	*w^{1118} ; ; P[w^+:UAS LacZ wg 3'UTR 355-1098 pAJS 402]*	LS1 Transgene	Mapped to chromosome III
258	*w^{1118} ; ; P[w^+:UAS LacZ wg 3'UTR 355-1098 pAJS 402]*	LS1 Transgene	Mapped to chromosome III
261	*w^{1118} ; ; P[w^+:UAS LacZ wg 3'UTR 355-1098 pAJS 402]*	LS1 Transgene	Mapped to chromosome III
262	*w^{1118} ; ; P[w^+:UAS LacZ wg 3'UTR 355-1098 pAJS 402]*	LS1 Transgene	Tested by FISH, mapped to chromosome III
277	*w^{1118} ; P[w^+:UAS LacZ wg 3'UTR 355-1098 pAJS 406]*	LS11 Transgene	Tested by FISH, mapped to chromosome II
289	*w^{1118} ; P[w^+:UAS LacZ wg 3'UTR 355-1098 pAJS 406]*	LS11 Transgene	Tested by FISH, mapped to chromosome III
400	*w^{1118} P[w^+:UAS LacZ wg 3'UTR 355-1098 pAJS 376]*	LS12 Transgene	Mapped to chromosome III
448	*w^{1118} P[w^+:UAS LacZ wg 3'UTR 355-1098 pAJS 376]*	LS12 Transgene	Tested by FISH, unmapped
457	*w^{1118} P[w^+:UAS LacZ wg 3'UTR 355-1098 pAJS 377]*	LS13 Transgene	Tested by FISH, unmapped
458	*w^{1118} P[w^+:UAS LacZ wg 3'UTR 355-1098 pAJS 377]*	LS13 Transgene	Unmapped
461	*w^{1118} P[w^+:UAS LacZ wg 3'UTR 355-1098 pAJS 377]*	LS13 Transgene	Unmapped
406	*w^{1118} ; ; P[w^+:UAS LacZ wg 3'UTR 355-1098 pAJS 378]*	LS14 Transgene	Tested by FISH, mapped to chromosome III
407	*w^{1118} ; P[w^+:UAS LacZ wg 3'UTR 355-1098 pAJS 378]*	LS14 Transgene	Tested by FISH, mapped to chromosome II
409	*w^{1118} P[w^+:UAS LacZ wg 3'UTR 355-1098 pAJS 378]*	LS14 Transgene	Mapped to chromosome I
410	*w^{1118} ; P[w^+:UAS LacZ wg 3'UTR 355-1098 pAJS 378]*	LS14 Transgene	Mapped to chromosome II
368	*w^{1118} ; P[w^+:UAS LacZ wg 3'UTR 355-1098 pAJS 407]*	LS15 Transgene	Tested by FISH, mapped to chromosome II
369	*w^{1118} ; ; P[w^+:UAS LacZ wg 3'UTR 355-1098 pAJS 407]*	LS15 Transgene	Mapped to chromosome III
370	*w^{1118} ; P[w^+:UAS LacZ wg 3'UTR 355-1098 pAJS 407]*	LS15 Transgene	Tested by FISH, mapped to chromosome II
371	*w^{1118} ; P[w^+:UAS LacZ wg 3'UTR 355-1098 pAJS 407]*	LS15 Transgene	Tested by FISH, mapped to chromosome II
402	*w^{1118} ; P[w^+:UAS LacZ wg 3'UTR 355-1098 pAJS 407]*	LS15 Transgene	Tested by FISH, mapped to chromosome II

Stock Number	Genotype	Source	Comment
265	w^{1118} ; P[w^+:UAS LacZ wg 3'UTR 355-1098 pAJS 408]	LS16 Transgene	Tested by FISH mapped to chromosome II
266	w^{1118} ; ; P[w^+:UAS LacZ wg 3'UTR 355-1098 pAJS 408]	LS16 Transgene	Tested by FISH, mapped to chromosome III
274	w^{1118} ; P[w^+:UAS LacZ wg 3'UTR 355-1098 pAJS 408]	LS16 Transgene	Mapped to chromosome II
451	w^{1118} P[w^+:UAS LacZ wg 3'UTR 355-1098 pAJS 418]	Δ15: LS1–LS12 deletion transgene	Unmapped
452	w^{1118} P[w^+:UAS LacZ wg 3'UTR 355-1098 pAJS 418]	Δ15: LS1–LS12 deletion transgene	Tested by FISH, unmapped
463	w^{1118} P[w^+:UAS LacZ wg 3'UTR 355-1098 pAJS 418]	Δ15: LS1–LS12 deletion transgene	Unmapped
468	w^{1118} P[w^+:UAS LacZ wg 3'UTR 355-1098 pAJS 418]	Δ15: LS1–LS12 deletion transgene	Tested by FISH, unmapped
450	w^{1118} P[w^+:UAS LacZ wg 3'UTR 355-1098 pAJS 364]	LS2 Transgene	Unmapped
453	w^{1118} P[w^+:UAS LacZ wg 3'UTR 355-1098 pAJS 364]	LS2 Transgene	Unmapped
459	w^{1118} P[w^+:UAS LacZ wg 3'UTR 355-1098 pAJS 364]	LS2 Transgene	Tested by FISH, unmapped
372	w^{1118} ; ; P[w^+:UAS LacZ wg 3'UTR 355-1098 pAJS 365]	LS3 Transgene	Tested by FISH, mapped to chromosome III
373	w^{1118} ; ; P[w^+:UAS LacZ wg 3'UTR 355-1098 pAJS 365]	LS3 Transgene	Tested by FISH, mapped to chromosome III
374	w^{1118} ; ; P[w^+:UAS LacZ wg 3'UTR 355-1098 pAJS 365]	LS3 Transgene	Tested by FISH, mapped to chromosome III
375	w^{1118} ; ; P[w^+:UAS LacZ wg 3'UTR 355-1098 pAJS 365]	LS3 Transgene	Mapped to chromosome III
376	w^{1118} ; ; P[w^+:UAS LacZ wg 3'UTR 355-1098 pAJS 365]	LS3 Transgene	Mapped to chromosome III
377	w^{1118} ; ; P[w^+:UAS LacZ wg 3'UTR 355-1098 pAJS 365]	LS3 Transgene	Mapped to chromosome III
401	w^{1118} ; ; P[w^+:UAS LacZ wg 3'UTR 355-1098 pAJS 366]	LS4 Transgene	Tested by FISH, mapped to chromosome III
403	w^{1118} ; ; P[w^+:UAS LacZ wg 3'UTR 355-1098 pAJS 366]	LS4 Transgene	Tested by FISH mapped to chromosome III
397	w^{1118} ; P[w^+:UAS LacZ wg 3'UTR 355-1098 pAJS 429]	Δ4: LS4-LS5 deletion transgene	Tested by FISH, mapped to chromosome II
251	w^{1118} ; P[w^+:UAS LacZ wg 3'UTR 355-1098 pAJS 403]	LS5 Transgene	Tested by FISH, mapped to chromosome II
252	w^{1118} ; P[w^+:UAS LacZ wg 3'UTR 355-1098 pAJS 403]	LS5 Transgene	Mapped to chromosome II
253	w^{1118} ; P[w^+:UAS LacZ wg 3'UTR 355-1098 pAJS 403]	LS5 Transgene	Tested by FISH, mapped to chromosome II
254	w^{1118} ; P[w^+:UAS LacZ wg 3'UTR 355-1098 pAJS 403]	LS5 Transgene	Mapped to chromosome II
255	w^{1118} ; ; P[w^+:UAS LacZ wg 3'UTR 355-1098 pAJS 403]	LS5 Transgene	Mapped to chromosome III
257	w^{1118} ; ; P[w^+:UAS LacZ wg 3'UTR 355-1098 pAJS 403]	LS5 Transgene	Mapped to chromosome III
268	w^{1118} P[w^+:UAS LacZ wg 3'UTR 355-1098 pAJS 403]	LS5 Transgene	Tested by FISH, mapped to chromosome I

Stock Number	Genotype	Source	Comment
466	w^{1118} P[w^+:UAS LacZ wg 3'UTR 355-1098 pAJS 404]	LS6 Transgene	Tested by FISH, unmapped
469	w^{1118} P[w^+:UAS LacZ wg 3'UTR 355-1098 pAJS 404]	LS6 Transgene	Unmapped
395	w^{1118} ; ; P[w^+:UAS LacZ wg 3'UTR 355-1098 pAJS 419]	Δ11: LS6-LS12 deletion transgene	Mapped to chromosome III
396	w^{1118} ; ; P[w^+:UAS LacZ wg 3'UTR 355-1098 pAJS 419]	Δ11: LS6-LS12 deletion transgene	Mapped to chromosome III
399	w^{1118} ; P[w^+:UAS LacZ wg 3'UTR 355-1098 pAJS 419]	Δ11: LS6-LS12 deletion transgene	Tested by FISH, mapped to chromosome II
398	w^{1118} ; ; P[w^+:UAS LacZ wg 3'UTR 355-1098 pAJS 372]	LS7 Transgene	Mapped to chromosome III
404	w^{1118} ; ; P[w^+:UAS LacZ wg 3'UTR 355-1098 pAJS 372]	LS7 Transgene	Tested by FISH, mapped to chromosome III
405	w^{1118} ; P[w^+:UAS LacZ wg 3'UTR 355-1098 pAJS 372]	LS7 Transgene	Tested by FISH, mapped to chromosome II
408	w^{1118} P[w^+:UAS LacZ wg 3'UTR 355-1098 pAJS 372]	LS7 Transgene	Unmapped
249	w^{1118} ; ; P[w^+:UAS LacZ wg 3'UTR 355-1098 pAJS 423]	Δ6: LS7-LS8 deletion transgene	Mapped to chromosome III
250	w^{1118} ; ; P[w^+:UAS LacZ wg 3'UTR 355-1098 pAJS 423]	Δ6: LS7-LS8 deletion transgene	Mapped to chromosome III
256	w^{1118} ; ; P[w^+:UAS LacZ wg 3'UTR 355-1098 pAJS 423]	Δ6: LS7-LS8 deletion transgene	Mapped to chromosome III
259	w^{1118} ; P[w^+:UAS LacZ wg 3'UTR 355-1098 pAJS 423]	Δ6: LS7-LS8 deletion transgene	Mapped to chromosome II
260	w^{1118} ; ; P[w^+:UAS LacZ wg 3'UTR 355-1098 pAJS 423]	Δ6: LS7-LS8 deletion transgene	Tested by FISH, mapped to chromosome III
263	w^{1118} ; P[w^+:UAS LacZ wg 3'UTR 355-1098 pAJS 423]	Δ6: LS7-LS8 deletion transgene	Mapped to chromosome II
264	w^{1118} ; ; P[w^+:UAS LacZ wg 3'UTR 355-1098 pAJS 423]	Δ6: LS7-LS8 deletion transgene	Tested by FISH, mapped to chromosome III
271	w^{1118} ; P[w^+:UAS LacZ wg 3'UTR 355-1098 pAJS 423]	Δ6: LS7-LS8 deletion transgene	Mapped to chromosome II
304	w^{1118} P[w^+:UAS LacZ wg 3'UTR 355-1098 pAJS 423]	Δ6: LS7-LS8 deletion transgene	Mapped to chromosome I
305	w^{1118} P[w^+:UAS LacZ wg 3'UTR 355-1098 pAJS 423]	Δ6: LS7-LS8 deletion transgene	Mapped to chromosome I
267	w^{1118} ; P[w^+:UAS LacZ wg 3'UTR 355-1098 pAJS 405]	LS8 Transgene	Tested by FISH, mapped to chromosome II
269	w^{1118} ; ; P[w^+:UAS LacZ wg 3'UTR 355-1098 pAJS 405]	LS8 Transgene	Mapped to chromosome III
270	w^{1118} ; ; P[w^+:UAS LacZ wg 3'UTR 355-1098 pAJS 405]	LS8 Transgene	Mapped to chromosome III
272	w^{1118} ; ; P[w^+:UAS LacZ wg 3'UTR 355-1098 pAJS 405]	LS8 Transgene	Mapped to chromosome III
273	w^{1118} ; P[w^+:UAS LacZ wg 3'UTR 355-1098 pAJS 405]	LS8 Transgene	Tested by FISH, mapped to chromosome II
275	w^{1118} ; ; P[w^+:UAS LacZ wg 3'UTR 355-1098 pAJS 405]	LS8 Transgene	Mapped to chromosome III
276	w^{1118} ; P[w^+:UAS LacZ wg 3'UTR 355-1098 pAJS 405]	LS8 Transgene	Mapped to chromosome II

Stock Number	Genotype	Source	Comment
278	*w^{1118} ; P[w^+:UAS LacZ wg 3'UTR 355-1098 pAJS 405]*	LS8 Transgene	Mapped to chromosome II
279	*w^{1118} ; ; P[w^+:UAS LacZ wg 3'UTR 355-1098 pAJS 405]*	LS8 Transgene	Tested by FISH, mapped to chromosome III
455	*w^{1118} P[w^+:UAS LacZ wg 3'UTR 355-1098 pAJS 373]*	LS9 Transgene	Unmapped
456	*w^{1118} P[w^+:UAS LacZ wg 3'UTR 355-1098 pAJS 373]*	LS9 Transgene	Tested by FISH, unmapped
465	*w^{1118} P[w^+:UAS LacZ wg 3'UTR 355-1098 pAJS 373]*	LS9 Transgene	Tested by FISH, unmapped
446	*w^{1118} P[w^+:UAS LacZ]*	Untagged LacZ transgene	Unmapped
447	*w^{1118} P[w^+:UAS LacZ]*	Untagged LacZ transgene	Unmapped
449	*w^{1118} P[w^+:UAS LacZ]*	Untagged LacZ transgene	Unmapped
454	*w^{1118} P[w^+:UAS LacZ]*	Untagged LacZ transgene	Unmapped
464	*w^{1118} P[w^+:UAS LacZ wg 3'UTR 659-775 pAJS 131 WLE2*	Wild-type WLE2	Tested by FISH, unmapped
460	*w^{1118} P[w^+:UAS LacZ wg 3'UTR 355-1098 pAJS 350]*	Wild-type WLE2-3	Unmapped
467	*w^{1118} P[w^+:UAS LacZ wg 3'UTR 355-1098 pAJS 350]*	Wild-type WLE2-3	Tested by FISH, unmapped

Fly cultures

D. melanogaster cultures were kept at temperatures ranging from 18°C to 28°C, depending on the desired rate of growth, and in concordance with standard culturing techniques. A list of all transgenic flies created for the purpose of this thesis can be found in Table 2-3. All other flies referred to in this thesis were ordered from the Bloomington Stock Centre.

Software

Basic adjustments to brightness, contrast and placement along with measurements were done with Adobe Photoshop CS, ImageJ version 1.38m (Abramoff, 2004), and Microsoft Office. Image acquisition on PerkinElmer spinning disc confocal microscope was done using Ultraview (2.1) software and Carl Zeiss AIM LSM Image (version) when using the LSM510 confocal microscope. Nucleotide alignments were performed using ClustalX version 1.83 under default conditions unless otherwise noted (Thompson et al., 1997). Alignments were visualized using Jalview version 2.07 (Clamp et al., 2004) or Geneious version 2.5.4 (Drummond AJ, 2006). RNA secondary structure was predicted using RNAstructure 4.4 (Mathews et al., 2004) and visualized using RNAdraw version 1.1b2 (Matzura and Wennborg, 1996). Video editing and frame captures were performed with VirtualDub version 1.6.16 build 24463. Plasmid visualization and manipulation was performed with Acaclone pDraw32 version 1.1.93 and DNA sequencing data was analyzed using Thechnelysium Chromas version 2.3.

Chapter 3
Results

WLE2 is not sufficient for apical localization

Like the vast majority of localized RNAs, the cis-acting sequences recognized by the transport machinery in *wg* are found exclusively in the 3' untranslated region (UTR) of the mRNA (Simmonds et al., 2001; St Johnston, 2005). These transport sequences have been mapped to three discrete regions named WLE1 (55-181), WLE2 (672-771) and more recently WLE3 (518-570) (Figure 1-1) (dos Santos, 2006; Simmonds et al., 2001).

To further our understanding of the sequences that direct the transport of RNA to specific domains of the cytoplasm, WLE2 was chosen as a candidate to define a consensus sequence necessary for apical localization of *wg* mRNA. WLE2 seemed like a better candidate to study this process because of the two WLEs known at the time, the apical localization conferred by WLE2 more closely resembled that of full length (FL) 3' UTR (Simmonds et al., 2001). To identify the critical nucleotides within WLE2, PCR mediated mutagenesis was used to introduce *Bgl*II restriction sites within the WLE2 sequence. These mutations were tested for their effect on apical localization using the direct injection assay. The direct injection assay allows real-time visualization of fluorescently labelled RNA injected into the embryonic blastoderm and offers an attractive alternative to time the consuming FISH assay (Glotzer et al., 1997; Lall et al., 1999).

Upon injection, the majority of *in vitro* transcribed, 5' capped, Alexa-Fluor labelled FL wild-type *wg* 3' UTR RNA sequence became tightly associated with the apical cortex of the syncytial blastoderm after 5 min, and by 10 min there was very little detectable unlocalized RNA. Surprisingly, injection of wild-type WLE2 RNA into the *Drosophila* blastoderm did not lead to the apical accumulation of the injected RNA like that seen of FL 3' UTR (Figure 3-1A-B). Injected WLE2 RNA can be visualized in the central blastoderm even after 15 min, suggesting that the lack of localization is indeed due to an inability to localize rather than the rapid degradation of the RNA before localization occur. The results obtained from WLE2 closely resemble those of the *wg* antisense ORF negative control (Figure 3-1C).

Figure 3-1: RNA transcribed from the minimal WLE2 sequence does not localize apically in the direct injection assay. Each frame represents a single slice from a 4-dimensional confocal stack at the time points indicated. Syncytial nuclei were marked with GFP (green). **A)** Fluorescently labelled RNA corresponding to FL *wg* 3' UTR sequence injected into syncytial embryos began to be transported to the apical cortex immediately after injection – the majority of the RNA was localized by 8 mins. **B)** Fluorescent WLE2 RNA showed no significant directional movement towards the apical cortex upon injection. **C)** A negative control with RNA sequence anti-sense to the *wg* ORF behaved similarly to WLE2.

The differences between the previously published data and the new data regarding the apparent localization activity of WLE2, raises the possibility that the direct injection assay was not representative of *in vivo* situations. While the direct injection assay provides a quick method of testing the localization capacity of a particular RNA sequence, it does not exactly mimic an *in vivo* based analysis such as FISH. To address this possibility, transgenic flies expressing the WLE2 sequence attached to a lacZ reporter under the control of a UAS promoter crossed to flies expressing Gal4 under an *en* promoter, and analyzed using FISH. Like *wg*, *en* is also expressed in a series of 14 stripes along the anterior-posterior axis of the *Drosophila* embryo (Baker, 1987; Fjose et al., 1985; Kornberg et al., 1985). However *wg* is expressed in the posterior compartment of each parasegment while *en* is expressed in the anterior compartment, therefore no cell expresses both of these genes (Figure 3-2A). Embryos derived from the above cross were therefore expressing the lacZ-WLE2 transgene in an *en* pattern and endogenous *wg* in a wild-type pattern. In agreement with the results obtained from direct injections, FISH showed that FL 3' UTR was able to localize the lacZ reporter in manner similar to endogenous *wg*, while the minimal WLE2 sequence was not sufficient to direct apical transport (Figure 3-2B-C).

Figure 3-2: WLE2 is not sufficient to localize a lacZ reporter sequence *in vivo*. FISH was done using probes against the lacZ (red) sequence and the *wg* ORF (green) in 3-5 hour old embryos.**B) – C)** Nuclei counterstained with wheat germ agglutinin were also included in the merged image (blue). The approximate outlines of one transgene-expressing cell and one *wg* expressing cell are outlined with a white dotted line. **A)** The lacZ transgene under the control of a UAS promoter is being expressed in an *en* pattern by using an *en*-Gal4 driver (red). Like endogenous *wg* mRNA (green), the lacZ reporter is expressed in a series of 14 stripes along the anterior-posterior axis of the embryo. Anterior is on the right and posterior on the left. **B)** Full length *wg* 3' UTR attached 3' to the lacZ reporter causes a majority of the lacZ transcripts to localize apical to the nuclei, and as expected, endogenous *wg* mRNA is also apically localized. **C)** LacZ RNA attached to WLE2 sequence does not lead to an accumulation of lacZ reporter RNA in the apical regions of the cell compared to endogenous *wg* mRNA localizes.

WLE2 can affect WLE3 localization

Since our data show that as a cis-acting sequence, WLE2 is not sufficient to direct apical transport, it became necessary to test the alternative hypothesis that the role of WLE2 is to modify or assist activity of other WLEs. The localization of WLE2 was tested in the presence of WLE3 (518-570), a region known to require downstream factors for its function (dos Santos, 2006). The effect of WLE2 on WLE3 was tested in the larger WLE2-3 construct (355-1098), which consists of all *wg* 3' UTR nucleotides downstream of 354. The WLE2-3 construct is able to localize apically when expressed as a UAS-lacZ tagged transgene or when injected directly into the syncytial blastoderm of *D. melanogaster* (Figure 3-4A, 3-5A and Table 3-1). To test if WLE2 was an accessory factor required for WLE3 mediated localization, a series of endonuclease digestions were performed on the WLE2-3 template used to transcribe the RNA for the direct injections. This produced a WLE2-3 construct that was sequentially truncated from the 3' end (Figure 3-3C). None of RNA sequences truncated downstream of WLE2 (*Ssp*I, *Dde*I and *Pac*I) nor those within the WLE2 sequence (*Hin*dIII and *Bsr*GI) had an effect on the transport of the WLE2-3 construct in the direct injection assay. Even the truncation that effectively removed the entire WLE2 sequence (*Sty*I) did not affect the ability of remaining sequence to localize apically (Table 3-1). Deletion of the WLE2 region also did not appear to affect transport rate of the remaining sequence, although subtle differences between various constructs may exist. Together with the previous results, our data suggest that WLE2 is neither sufficient nor necessary to direct apical transport.

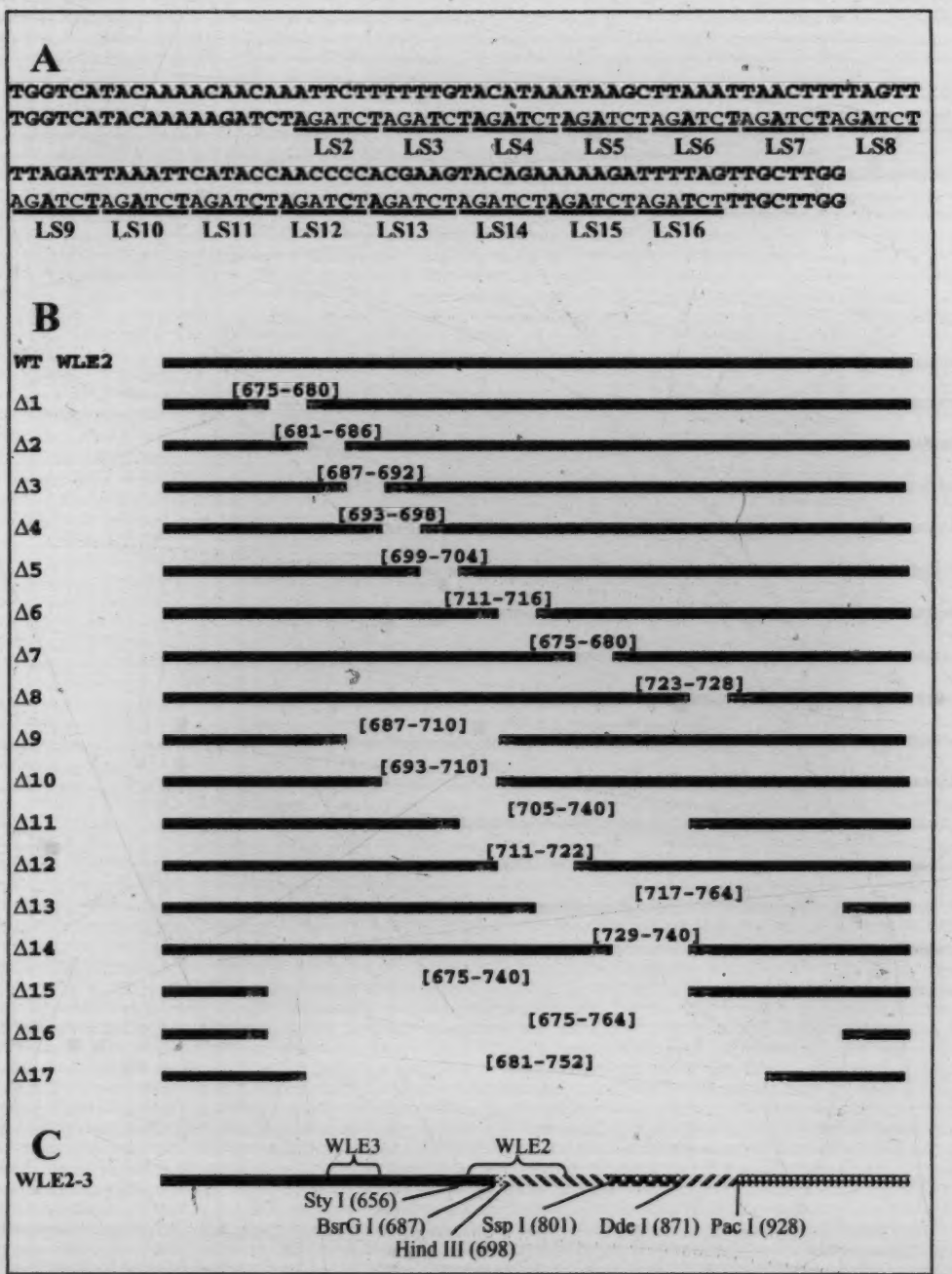

Figure 3-3: Mutations in WLE2 and downstream regions tested for localization defects. A) Shows the bases mutated using linker scanner mutagenesis and their corresponding names. In the pairs of sequences, the top sequence shows wild-type WLE2 (659-775) while the bottom sequence shows what the wild-type sequence has been mutated to. In the bottom strand, orange coloured bases indicate that replacement of a 6 nucleotide region has altered the sequence of that base from wild-type, while black bases indicate that the nucleotide remained unchanged after mutagenesis. Each LS mutation is only mutant in the bases that have been underlined, and nucleotides upstream and downstream are of wild-type WLE2 sequence. All the LS results shown were obtained using a WLE2-3 construct. **B)** Shows a scaled schematic of the deletions

created along the length of the WLE2 region by digesting and ligating various linker scanner mutations. For example, Δ1 was obtained by digesting LS1 and LS2 with *Bgl*II and ligating them to one another. This results not only in a deletion but also changes the three bases upstream and downstream of the deletion into AGA and TCT respectively. Where the change results in a deviation from the wild-type sequence, the altered bases have been coloured white. These deletions were only tested in a WLE2-3 (355-1098) context. **C)** Shows a scaled schematic of the relative locations of restriction enzyme recognition sites used in sequential digests of the 744 nucleotide WLE2-3. Restriction enzyme sites correspond to nucleotide numbers in FL 3' UTR, however, only the WLE2-3 region is shown in the schematic.

Table 3-1: Mutations in WLE2 can influence the apical transport of the WLE2-3 constructs. Fluorescent RNA transcribed off WLE2-3 templates truncated by digestion with the indicated enzymes, or mutated using linker scanner mutagenesis (Figure 3-3) was injected into syncytial embryos and visualized using 4D confocal microscopy. A ** denotes localization identical to the wild-type WLE2-3 sequence, while a - indicates no apparent transport of the RNA towards the periphery. Constructs marked by a * appear to display some directed movement towards the periphery but do not reach the apical cortex. Instead, they appear to be enriched basally.

Construct	Localization	Construct	Localization
Xho I (355-1098)	**	**LS15**	**
Pac I (355-928)	**	**LS16**	**
Dde I (355-871)	**	**Δ1**	**
Ssp I (355-801)	**	**Δ2**	**
Hind III (355-698)	**	**Δ3**	-
BsrG I (355-687)	**	**Δ4**	**
Sty I (355-656)	**	**Δ5**	**
LS2	**	**Δ6**	**
LS3	**	**Δ7**	*
LS4	**	**Δ8**	**
LS5	**	**Δ9**	**
LS6	**	**Δ10**	**
LS7	**	**Δ11**	**
LS8	**	**Δ12**	**
LS9	**	**Δ13**	**
LS10	**	**Δ14**	**
LS11	*	**Δ15**	**
LS12	**	**Δ16**	**
LS13	**	**Δ17**	-
LS14	**		

Since previous research has suggested that WLE3 requires additional downstream factors for normal function, and that subtle changes within these sequences result in aberrant localization (dos Santos, 2006), we tested the effect of small mutations in the WLE2 sequence on WLE3. To do this, we used linker scanner (LS) mutagenesis – a PCR mediated mutagenesis method most often used to identify essential bases in gene promoters – to introduce a series of mutations along the length of WLE2. These mutations changed the wild-type WLE2 sequence to a *Bgl*II restriction site (AGATCT) every six nucleotides, but left the remainder of the WLE2-3 construct unchanged (Figure 3-3A). The localization capacity of each LS mutated WLE2-3 construct was tested by direct injection (Table 3-1). The majority of the mutations within the WLE2 sequence had no visible effect on WLE2-3 localization (Figure 3-4A-B). However, the LS11 and Δ7 mutations were able to partially disrupt RNA transport (Figure 3-4C). The WLE2-3 RNA sequence containing the Δ7 mutation displayed some directional transport towards the embryonic periphery, but appeared to remain on the basal side of the nuclei lining the embryonic blastoderm. The LS11 mutation in the WLE2-3 construct was occasionally able to reach the apical cortex, but most often displayed a pattern similar to Δ7, where the injected RNA became concentrated basal to the nuclei with very little transported apically. This partial disruption of localization could be due to a conformational change, within WLE3 or other sequences, which results in a lower affinity to the localization machinery responsible for the recognition of the RNA structure. However, analysis of the *in silico* predicted secondary structures of the Δ7 and LS11 mutations shows no apparent influence on the secondary structure of WLE3. While both mutations alter the terminal loop of the WLE2 region, the stem of WLE2 and all sequence downstream and upstream are unaffected.

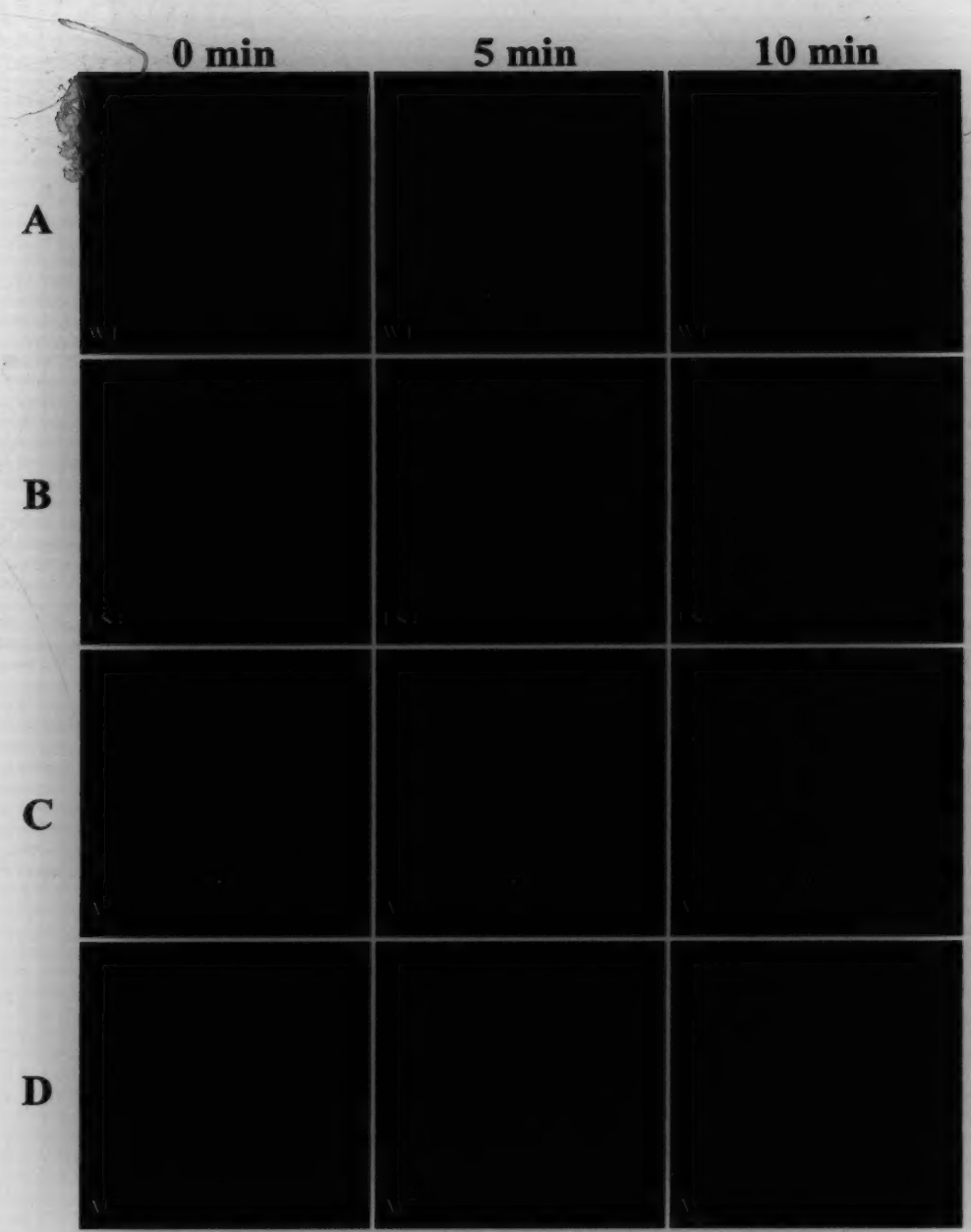

Figure 3-4: Mutations in WLE2 can affect the apical transport of WLE2-3 injected into syncytial embryos. *In vitro* transcribed, fluorescently labelled WLE2-3 (355-1098) (red) was injected into syncytial embryos expressing nuclear GFP (green). The transport of the RNA was visualized in real-time using confocal microscopy. Frame captures were then taken at the labelled time points from each time-lapse video. **A)** Wild-type WLE2-3 sequence. The large circle seen outside of the embryo is fluorescently labelled RNA that was ejected from the needle prior to injection of the embryo to ensure the needle was not plugged. **B)** The LS4 mutation of WLE2 in the WLE2-3 construct localizes normally. **C)** The Δ7 deletion of WLE2 shows directional movement of the RNA towards the apical cortex, however the RNA is accumulated basal to the nuclei. **D)** The Δ17 mutation of WLE2 displays no directionality in its movement.

Two other mutations had a more drastic effect on transport of the WLE2-3 sequence. The Δ3 and Δ17 mutations completely abolished any transport of the injected RNA. In both cases, some of the injected RNA rapidly diffused throughout the cytoplasm, while a large portion of the RNA formed very large aggregates that oscillated on the spot, but failed to display any directional movement towards any embryonic pole (Figure 3-4D). Analysis of the predicted secondary structures of these two deletions shows that both may alter the secondary structure of the RNA to a greater degree than the Δ7 and LS11 mutations. The larger Δ17 deletion effectively deletes WLE2, leaving only the proximal region of the stem intact, but has little impact on downstream structures or that of WLE3. Surprisingly, the smaller Δ3 deletion alters the conformation of the WLE2-3 construct almost entirely, forcing a smaller than normal WLE3 stem-loop structure and changing the structure of the supporting sequence drastically.

In order to verify the results of the direct injection assay, many of the LS mutations were also tested using FISH. Similar to the direct injection results, wild-type WLE2-3 was able to localize apically, as on average, greater than 45% of the RNA seen in each confocal slice was observed in the apical region of the cell (Figure 3-5A, Table 3-2). Most LS mutations examined appeared to have no impact on the apical localization of the WLE2-3 construct (Figure 3-5B, Table 3-2), but the LS2 and LS11 mutations appeared to reduce the localization of the WLE2-3 construct, as less than 45% but greater than 40% of observed RNA was found in the apical region (Figure 3-5C). The FISH results show that the LS5 mutation appears to completely abolish the localization activity of the WLE2-3 construct as less than 40% of the RNA is observed in the apical region (Figure 3-5D).

Both the direct injection and FISH results suggest that mutations in WLE2 can influence the localization of the WLE2-3 construct.

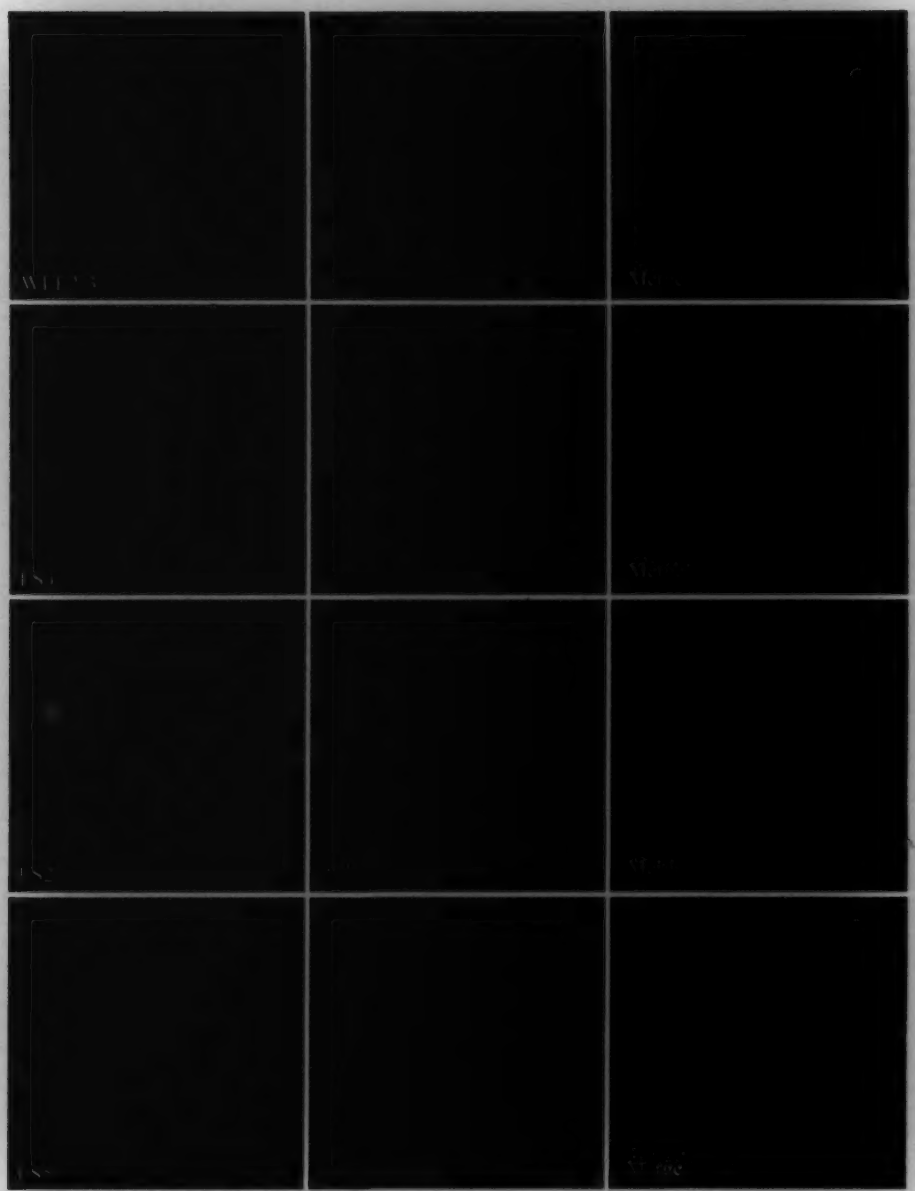

Figure 3-5: Mutations in WLE2 can affect the apical transport of the WLE2-3 construct *in vivo*. FISH performed on Lac-Z tagged wild-type and mutated WLE2 sequences expressed in an *en* pattern using the UAS/Gal4 system (red) and endogenous *wg* transcripts (green). Nuclei were counterstained with WGA (blue). In each merge, the approximate outline of a cell expressing the transgene and a cell expressing endogenous *wg* is shown with a white dotted line. **A)** Wild-type WLE2-3 sequence (355-1098) tagged to a lacZ reporter results in apical localization of the transcripts. **B)** The LS4 mutation, along with most other LS mutations, result in the apical localization of greater than or equal to 45% of the transcripts. **C)** The LS2 mutation, along with a few other LS mutations have a decreased ability to localize LacZ reporter sequence apically, as less than 45% but greater than 40% of the RNA localizes. **D)** The LS5 mutation completely disrupts the apical localization of the reporter gene, resulting in a uniform distribution of the RNA.

Table 3-2: FISH results show that WLE2 can influence WLE3 mediated localization in the WLE2-3 construct. FISH was performed to confirm some of the direct injection results. The results obtained from the FISH experiments were sorted into three categories. Single nuclei in confocal sections were divided into equal apical, middle and basal regions. An integrated density value was used as a measure of the amount of RNA present in each region as a proportion of total RNA present in that particular cell. If on average, >45% of the RNA was apical, it was categorized as **, while an apical population consisting of <45% but >40% of total RNA was categorized as * and a <40% apical RNA distribution is indicated by -.

Construct	FISH
FL	**
WLE2-3	**
WLE2	-
LS1	**
LS2	*
LS3	**
LS4	**
LS5	-
LS6	**
LS7	**
LS8	**
LS9	**
LS11	*
LS13	**
LS14	**
LS15	**
LS16	**
Δ4	**
Δ6	**
Δ11	**
Δ15	**

WLE2 is involved in multimerization

Since the previously published data had shown that WLE2 had the potential to localize (Simmonds et al., 2001), it seemed likely that it was somehow involved in localization, although it may not be acting directly as a cis-acting localization sequence as previously thought. The 3' UTR of many other localized RNAs have been shown to contain multiple redundant regions sufficient for transport of the transcript or multiple regions responsible for different aspects of localization such as translational suppression, localization during different stages of development or acting as flexible linkers (Brunel and Ehresmann, 2004; Dalby and Glover, 1993; Gautreau et al., 1997; Kim-Ha et al., 1993; Kislauskis et al., 1994; Lantz and Schedl, 1994; Macdonald and Kerr, 1997). In genes such as *bcd* (Ferrandon et al., 1997; Wagner et al., 2001), *h* (Bullock et al., 2003) and *osk* (Hachet and Ephrussi, 2004), regions within the 3' UTR have been implicated in the formation of RNA-RNA homodimers important for localization. To test whether WLE2 is performing a similar function, simultaneous injections of two different RNAs were performed. Each RNA was labelled with a different fluorophore in order to follow the movement of both RNAs simultaneously. As before, WLE2 sequence alone did not have the capacity to localize by itself (figure 3-6A), however, co-injection of wild-type WLE2 sequence with FL *wg* 3' UTR RNA sequence led to the apical accumulation of both transcripts (figure 3-6B). This suggests that the WLE2 sequence is being co-transported with FL 3' UTR. Co-transport of WLE2 is also observed when it is co-injected with WLE2-3, however the apical accumulation of WLE2 appears to be somewhat diminished in this combination (figure 3-6C). It is unlikely that these interactions are random, or the result of intermolecular interactions between the fluorophores, because co-injection of a lacZ ORF sequence with FL 3' UTR leads to the transport of the FL sequence only (figure 3-6D). Furthermore, simultaneous injection of anti-sense WLE2 and FL sequence leads to a strong apical localization of both transcripts as WLE2 is expected to anneal to the sense WLE2 region of the FL fragment through complimentary base pairing, suggesting that RNA-RNA interactions are sufficient for co-transport of an otherwise non-localized transcript (figure 3-6E). In all cases where co-transport of two different RNAs was observed, foci containing both RNAs were present both during transport and once the RNAs had reached their final destinations. This

supports the model that these large foci are composed of heterogeneous mixtures of multiple RNAs and proteins, and that localized RNAs share their transport machinery (Bullock et al., 2003; Wilkie and Davis, 2001).

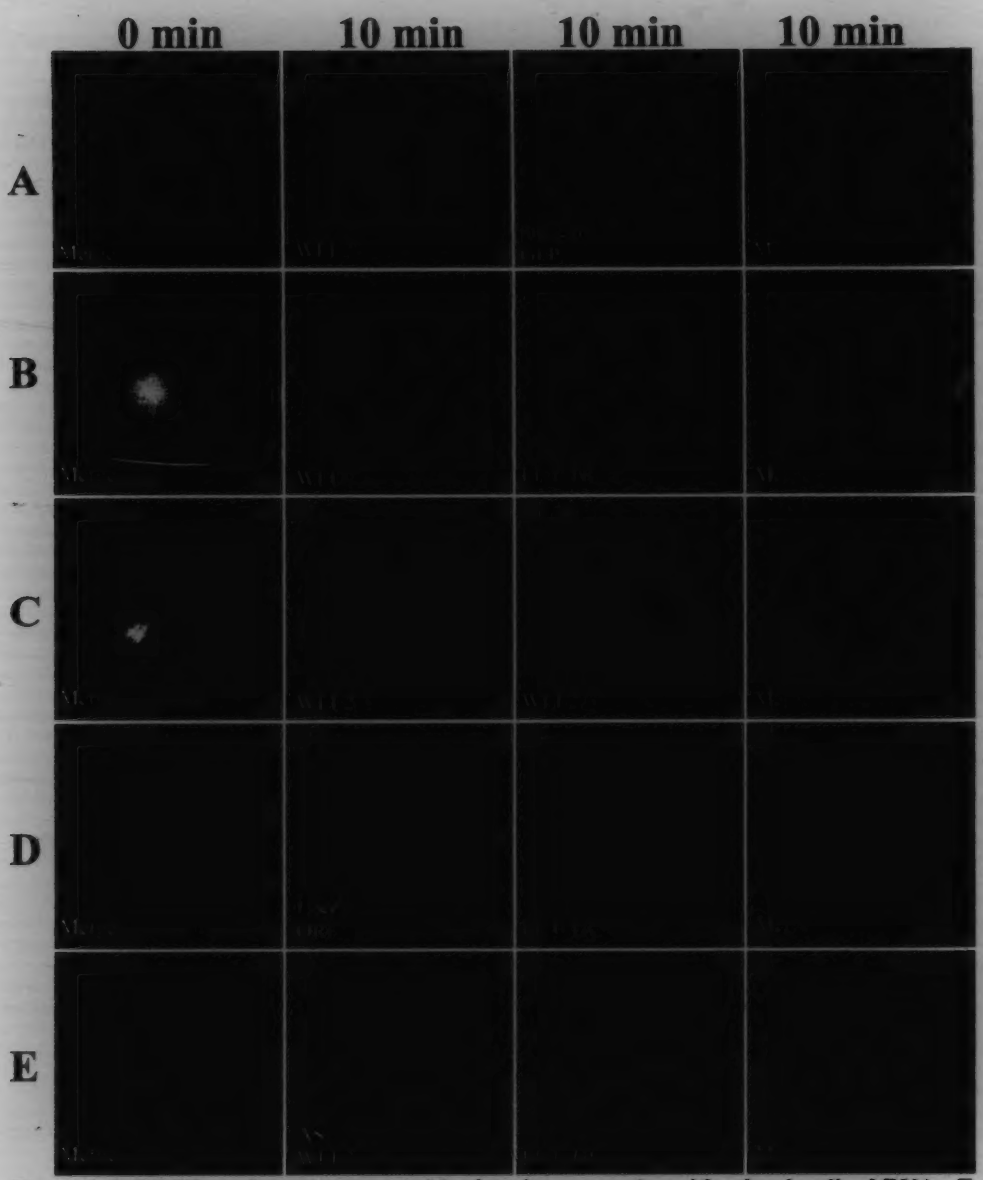

Figure 3-6: WLE2 can be co-transported by forming a complex with other localized RNAs. Two different RNA sequences, each labelled with a different fluorophore, were co-injected into syncytial embryos and visualized using 4D confocal microscopy. The first column shows a colour composite of both RNAs immediately after injection (time 0), the second column shows the distribution of one RNA sequence after 10 minutes, while the third column shows the location of the second injected sequence. The fourth column is a composite of both sequences after 10 minutes. **A)** Wild-type WLE2 RNA (red) was injected into embryos expressing nuclear GFP (green). **B)** WLE2 RNA (green) was co-injected with FL *wg* 3` UTR sequence (red), which resulted in the apical localization of both transcripts after 10 minutes. **C)** Co-injection of WLE2 (red) and WLE2-3 (green) also resulted in apical localization of both transcripts, although WLE2 localized to a lesser extent when injected with WLE2-3 as opposed to FL. **D)** LacZ ORF RNA (red) was co-injected with FL 3` UTR sequence (green) as a negative control. The FL transcripts were transported apically while the LacZ sequence diffused throughout the cytoplasm. **E)** RNA sequence anti-

sense to WLE2 was co-injected with sense FL RNA as a positive control, resulting in strong apical accumulation of both RNAs.

Chapter 4
Discussion

The necessity of RNA localization

Subcellular localization of mRNA is now recognized to be critical in the function of many genes. β-actin is localized to the distal lamellae of migrating chicken fibroblasts in order to ensure local production of actin protein where it is needed most, and prevent premature polymerization, or polymerization with different actin subunits during transport (Hill and Gunning, 1993; Lawrence and Singer, 1986). Delocalizing the actin transcripts causes a loss of cellular asymmetry and motility normally seen in these cells (Kislauskis et al., 1994; Kislauskis et al., 1997). RNA localization is also important in preventing ectopic expression of proteins in regions of a cell where it would be detrimental. One example of this is the Ash1 gene in *Saccharomyces cerevisiae*. Its RNA is restricted to the distal tip of budding yeast cells where it inhibits mating type switching in daughter cells, but can not function in the mother cell (Long et al., 1997; Takizawa et al., 1997). Transcript segregation to prevent ectopic expression is also observed in *D. melanogaster* embryos, where the first 13 divisions after fertilization are syncytial and therefore the nuclei lack plasma membranes that normally function to restrict the influence of transcription factors by preventing their diffusion into surrounding cells. Spatial organization of the mRNAs coding for early morphogens leads to a gradient of protein originating from the source transcripts. Localization of mRNA instead of the protein is also more efficient for the cell, as a single copy of mRNA can give rise to multiple copies of the corresponding protein, which do not each need to be transported. There are also, as yet, unknown reasons for the subcellular localization of certain transcripts. For instance, the transcripts of pair-rule genes *h, even-skipped* and *fushi tarazu* are actively transported by dynein, via microtubules, to a region apical to nuclei in the blastoderm (Davis and Ish-Horowicz, 1991; Lipshitz and Smibert, 2000; Wilkie and Davis, 2001). It has been proposed that the invaginating membrane of the cellularizing embryo prevents lateral diffusion of these transcripts allowing for sharp boundaries of activity (Davis and Ish-Horowicz, 1991). However, for localized transcripts such as *wg*, localization of transcripts to the apical region in order to prevent lateral diffusion is unnecessary, since *wg* is not expressed until after cellularization, where cellular membranes will ensure that the protein product does not enter the surrounding cells (Baker, 1987; Baker, 1988). In addition, if apical localization of *wg* transcripts was

necessary to prevent diffusion, one would expect a gain of function effect if the transcripts were evenly distributed throughout the cell, yet it has been shown that delocalizing the mRNA causes a loss of function phenotype. This suggests that although *wg* transcript localization is not required to prevent lateral diffusion, it is essential for gene function and not a remnant of evolution (Simmonds et al., 2001). The reasons for the necessity of *wg* transcripts in the apical region of the cell are not clear, however it is unlikely that ER resident proteins such as *porcupine*, implicated in palmitoylation of *Wg* may require an apically localized transcript (Kadowaki et al., 1996; Tanaka et al., 2002). Only one other gene is known to be essential in *Wg* secreting cells. *evenness interrupted* (*evi*) or *wntless* (*wls*) is a recently discovered seven pass trans-membrane protein implicated in the secretion of *Wg* (Banziger et al., 2006; Bartscherer et al., 2006). The studies differ with respect to the subcellular localization of Wls, where one study shows *wls* associated with the plasma membrane, while the other shows *wls* associated with the ER and the Golgi. As the studies disagree on the subcellular localization of Wls, the idea that it may require apically localized *wg* mRNA to function is unlikely due to the fact that *wls* mutants show defects in *Wg* secretion (Banziger et al., 2006; Bartscherer et al., 2006), whereas disruption of the apical localization of *wg* mRNA appears to increase Wg secretion, albeit in a non-functional form (Simmonds et al., 2001) . Due to the limited number of genes identified upstream of Wg receiving cells, it is likely that factors which require an apically localized transcript are general factors not specific to the *wg* pathway, and thus, the primary effects of mutations within these genes may not be easily associated with disruption of the *wg* pathway.

The mechanisms of RNA localization

Equally important as the necessity for localizing mRNA to specific sub-domains of cells, are the mechanisms by which transcripts are localized. There are four basic mechanisms which cells use to localize transcripts: local synthesis, selective degradation and protection, diffusion and entrapment and active motor protein based transport (reviewed, St Johnston, 2005). A number of trans-acting factors have been identified in mRNA trafficking, including motor proteins such as dynein (Schnorrer et al., 2000; Wilkie and Davis, 2001), kinesin (Carson et al., 1997) and myosin (Long et al., 1997),

along with proteins such as *Bicaudal-D/ egalitarian* that may be acting as adapters between the RNA cargo and the motor proteins (Mach and Lehmann, 1997; Navarro et al., 2004) and proteins such as She2p (Bohl et al., 2000), ZBP1 (Ross et al., 1997), hnRPA A2 (Hoek et al., 1998) and *stuafen* (Ferrandon et al., 1994; Ramos et al., 2000) that are believed to recognize and bind to the cis-acting sequences that direct mRNA trafficking.

Since many of these trans-acting factors are implicated in the transport of multiple RNAs, it is assumed that there are common transport pathways that are shared by a variety of localized RNAs. Further evidence for this comes from studies which show that localized maternal transcripts that are normally observed only in the oocyte, such as *bcd, nos, grk* and *K10*, have the potential to localize apically when injected into the *Drosophila* blastoderm despite not normally being expressed during that time in development (Bullock and Ish-Horowicz, 2001). In addition, injection of two different transcripts results in the formation of large heterogeneous RNA complexes that co-transport both transcripts (Wilkie and Davis, 2001). Yet, despite being transported in the same RNP complexes, there have been no apparent structural or sequence similarities that would unite groups of localized RNAs. It is hoped that as more localized RNAs are discovered, and their cis-acting localization signals determined, a consensus sequence or structure can be derived in order to further understand the mechanisms by which cells transport RNAs.

WLE2 does not act as a cis-acting localization signal

With minor exceptions, most RNA transport signals are found within the 3' UTR, and in the case of *wg*, there are three regions within the 3` UTR implicated in the transport of the RNA (dos Santos, 2006; reviewed, Kloc and Etkin, 2005; Simmonds et al., 2001). The focus of this thesis is to identify the role played by WLE2 in the apical localization of *wg* mRNA in polarized epithelial cells of the *Drosophila* embryo. WLE2 was previously shown to be one of two cis-acting localization signals necessary to transport *wg* RNA and reporter genes cloned 5' to it, to the apical cortex of the cellular blastoderm (Simmonds et al., 2001). The results presented here suggest that the minimal WLE2 region is not sufficient to direct apical transport when injected into the blastoderm.

Since WLE2 was previously believed to be sufficient for apical localization, it was important to exclude the possibility that these results were due to limitations with the direct injection assay. It is possible that the covalent linking of large fluorophores required for the direct injection assay may inhibit the formation of normal secondary structure associated with the sequence, or that the factors responsible for recognizing WLE2 are not present during the developmental period when the labelled RNA is injected. Both of these issues were addressed by performing FISH on embryos expressing a lacZ-WLE2 transgene in an *en* pattern. WLE2 still failed to localize apically in this situation, suggesting that it is not sufficient to direct transport of a reporter sequence.

It was also shown that WLE2 is not necessary to direct apical localization as fluorescent transcripts, sequentially deleted from the 3' end of the WLE2-3 construct, showed no apparent differences in localization from the wild-type WLE2-3 construct when WLE2 or any other sequences downstream of nucleotide 656 in the 3' UTR were removed. There exists the possibility that the minimal WLE2 sequence, like WLE3 (dos Santos, 2006), is not sufficient for localization but requires the presence of downstream sequences. This possibility has not yet been excluded, and to do so requires testing of WLE2 fused to downstream sequences by creating a construct that spans nucleotides 659-1098 of the *wg* 3' UTR. The results from this construct will not be confounded by the presence of WLE3 and any apical localization seen will likely be due to WLE2. If WLE2 is able to localize within this construct, sequential deletion from the 3' end will identify the minimal length of downstream accessory sequence needed for WLE2 function.

In the larger construct that we tested, which spanned nucleotides 355-1098 in the 3' UTR, named WLE2-3, apical localization was likely mediated by WLE3. WLE3 (518-570) was identified by our collaborators as a region upstream of WLE2 that is sufficient for apical localization in both the direct injection assay and FISH (dos Santos, 2006). In that study, the WLE2 region is identified as one of many interchangeable accessory sequences required for WLE3 function. We show that no more than the first 86 nucleotides directly downstream of WLE3 (which excludes WLE2) are required for the WLE2-3 construct to localize, while their results show that the first 90 nucleotides are not sufficient to allow WLE3 mediated RNA transport. This discrepancy could be explained by considering that our construct consisted of nucleotides 355-656 from the *wg* 3' UTR,

while theirs was comprised of only the WLE3 sequence and 90 bases directly downstream of it and containing no nucleotides 5` to it (518-660). Since it is believed that the structure of WLE3 is important in its recognition by the trafficking machinery, it is possible that in our construct, the additional sequence upstream of WLE3 helped it form the correct secondary structure required for its localization function. It is also possible that extra 4 downstream nucleotides included in their construct (657-660) rendered the conformation of WLE3 unrecognizable by the trans-acting recognition factors. Indeed, computer models of the predicted secondary structures show that the conformation of WLE3 is different between our construct and those of dos Santos (Figure 4-1). In our larger 355-656 construct, RNA sequence upstream of WLE3 appears to loop around and base pair with downstream sequences. This drastically changes the conformation of the sequences that flank WLE3 and possibly allows the binding of trans-acting factors that are excluded from the smaller construct. It also has an impact on the proximal stem of WLE3, where the opposite strands of the double-stranded stem have a bulge (Figure 4-1C). The predicted conformation of WLE3 in our construct is identical to the predicted conformation it has in the wild-type WLE2-3 construct, which supports the hypothesis that the conformational change predicted in the dos Santos construct is responsible for its lack of localization (Figure 4-1, 4-2, 4-3).

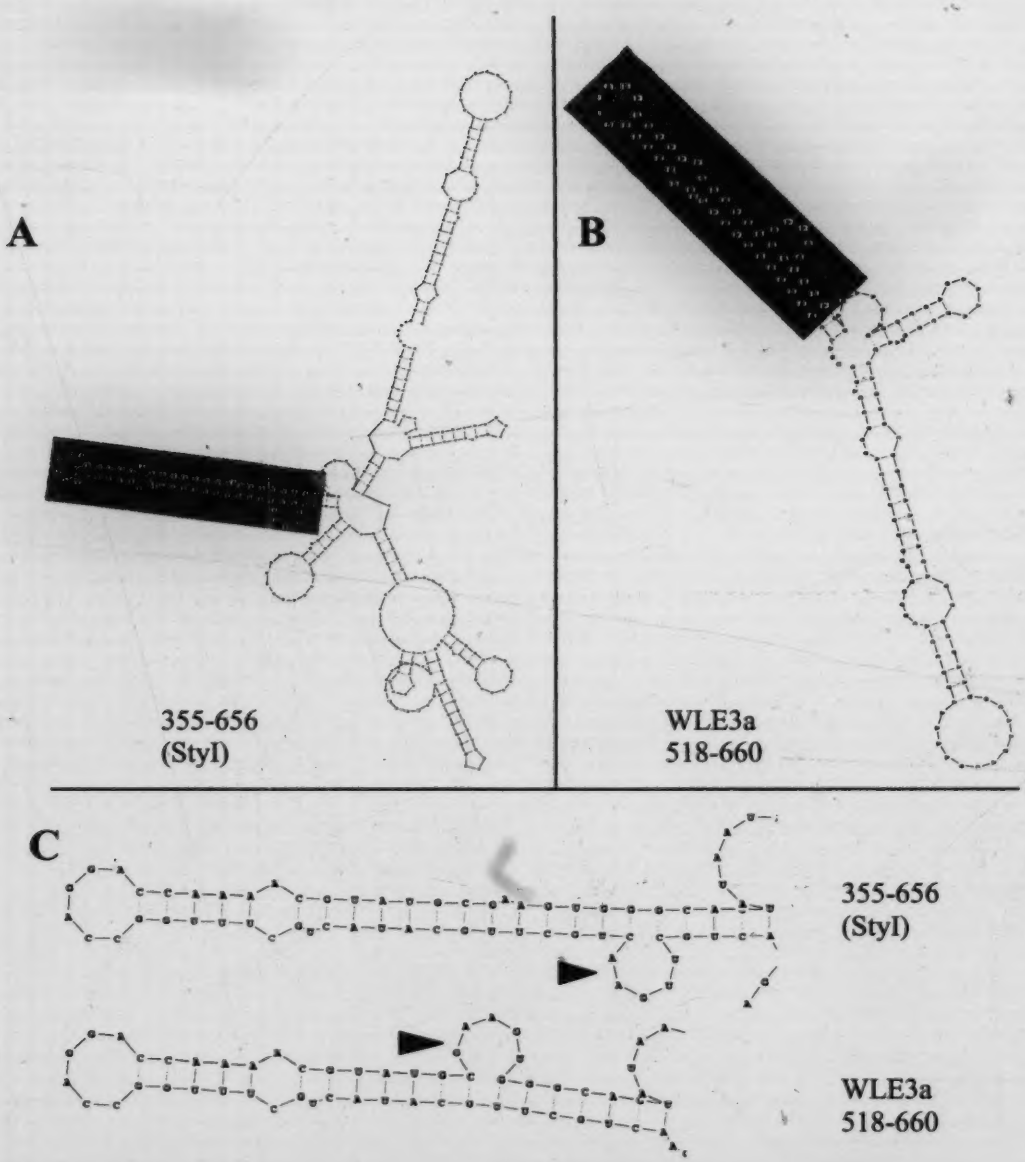

Figure 4-1: The secondary structure of WLE3 is affected by upstream and downstream sequences. A) The predicted structure of the WLE2-3 sequence truncated to the site of the *StyI* restriction site at position 656. **B)** The predicted structure of the WLE3a construct from dos Santos (2006). The grey insets from panels A and B highlight the WLE3 region in both constructs, and have been enlarged to display detail in panel C. Arrows point out differences between the two WLE3 regions. Both secondary structures were calculated at 25°C.

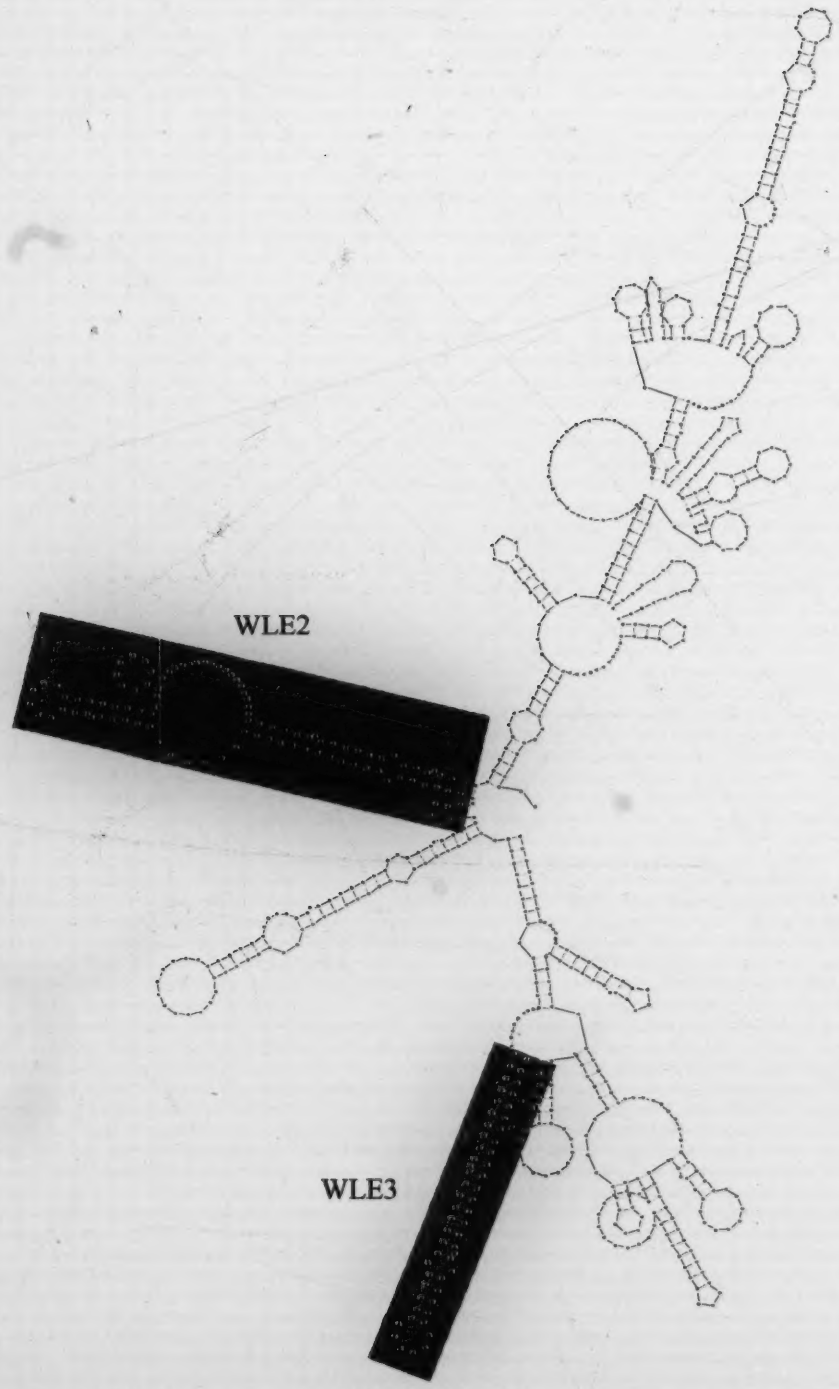

Figure 4-2: Predicted structure of the wild-type WLE2-3 sequence. Computer predicted model of the WLE2-3 (355-1098) sequence at 25°C. Grey boxes highlight the WLE2 and WLE3 regions

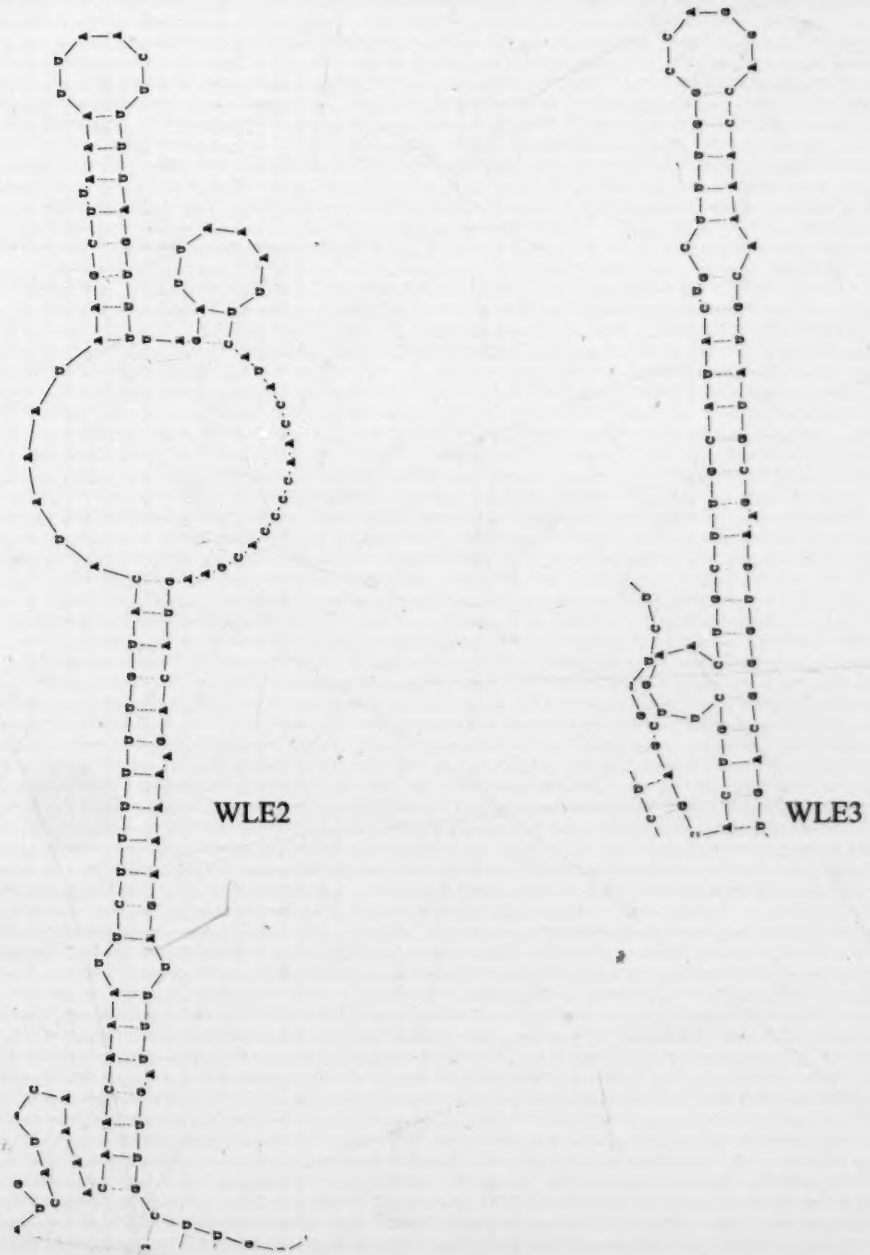

Figure 4-3: Magnified views of wild-type WLE2 and WLE3 in the WLE2-3 construct. Structures of WLE2 and WLE3 at 25°C were computed in the larger WLE2-3 construct comprising of nucleotides 355-1098. These are magnified versions of the grey insets in figure 4-2.

WLE2 influences WLE3 structure and function

It is unlikely that the only function of WLE2 is a passive role as a potentiator of WLE3 function. At the very least, it helps WLE3 assume a proper secondary structure, and the strong secondary structure of WLE2 itself likely acts as a boundary element and shields WLE3 from the influences of downstream sequences on the secondary structure of WLE3. The sensitivity of WLE3 to downstream sequences is further supported by our results, which show that mutations within WLE2 can effectively knock out or reduce WLE3 induced transport. Both LS11 and Δ7 appear to reduce localization activity of WLE3. After injection of these mutant WLE2-3 sequences, the RNA does display some directional transport towards the peripherally situated nuclei, but stops and accumulates basally once it reaches them. It appears as if the RNA can not cross the basal plane to reach the apical cortex. Analysis of the predicted structures caused by these two mutations shows that WLE3 is unaffected by either (Figure 4-4, 4-5). Both mutations only seem to affect the distal stem loop of WLE2 with no downstream or upstream effect. It is possible these mutations could have subtle influences on the conformation of WLE3 not accurately modelled by the secondary structure calculation algorithms. It is also possible that they induce changes in the tertiary structure of pseudoknots that may have a smaller impact on transport. If WLE3 is recognized by multiple trans-acting factors, each partially responsible for its localization, then these mutations could alter the conformation such that it is recognized by some factors and not others, leading to a partial disruption of localization.

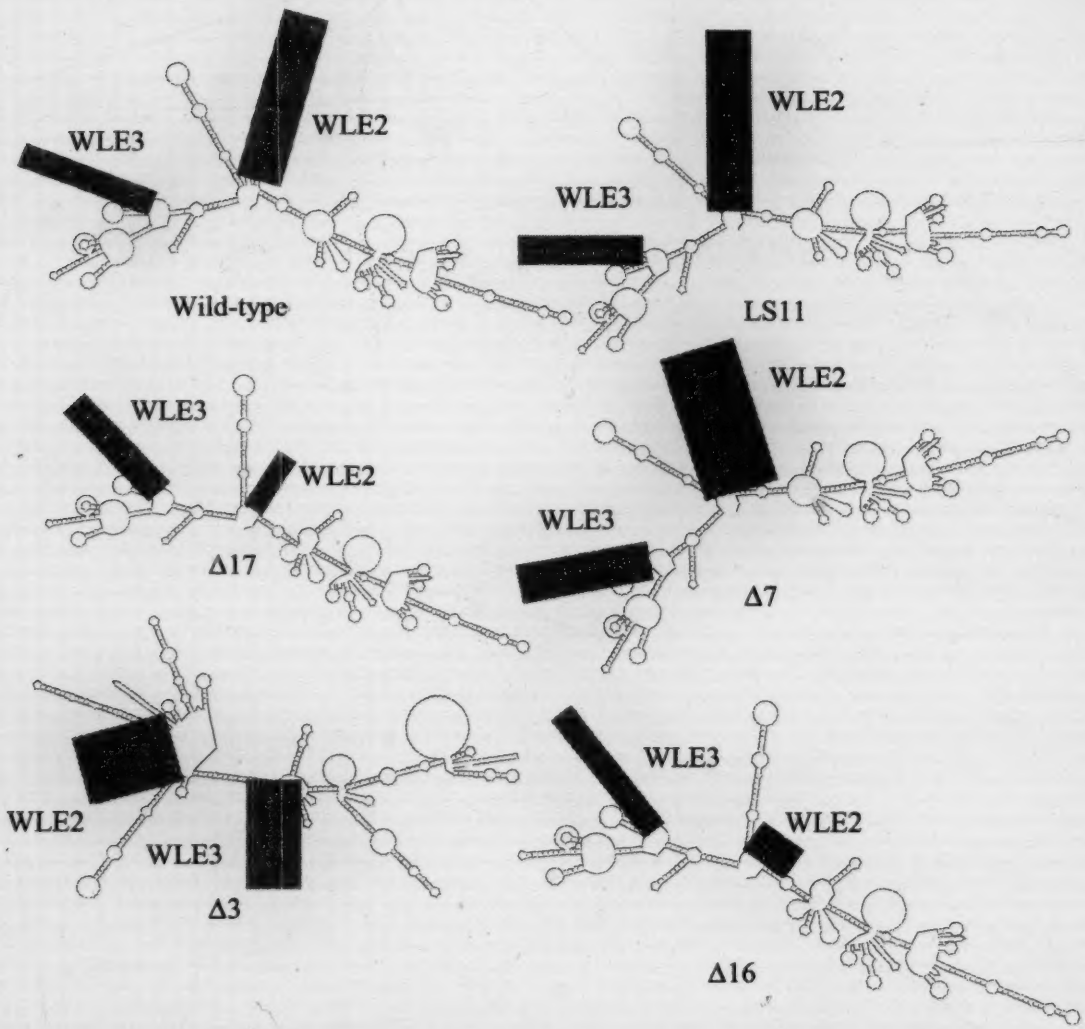

Figure 4-4: The predicted structures of the wild-type WLE2-3 sequence compared to those of mutations LS11, Δ17, Δ7, Δ3 and Δ16. A side by side comparison of the predicted structures of several key mutations in the WLE2-3 construct at 25°C. Magnified versions of LS11 and Δ7 are shown in Figure 4-5, and Δ17 and Δ3 in Figure 4-6. The regions corresponding to WLE2 and WLE3 are highlighted in grey.

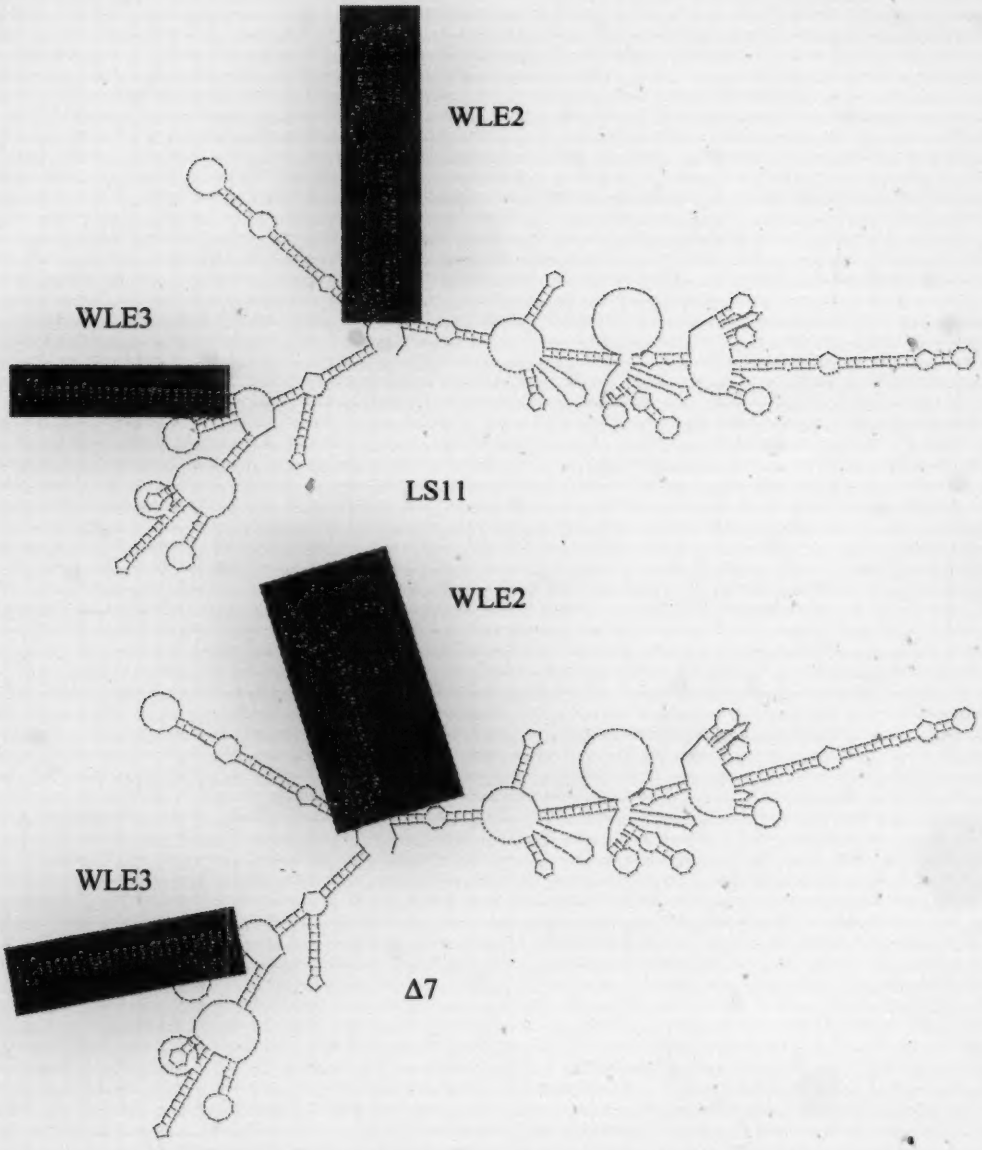

Figure 4-5: The predicted structures of the LS11 and Δ7 mutations. Computer predicted structures of the mutations that appear to reduce the capacity of the WLE2-3 construct to localize at 25°C. The WLE2 and WLE3 regions have been highlighted in grey.

Analysis of the predicted secondary structures of the two mutations that completely abolished transport of the injected WLE2-3 construct showed that the larger of the two deletions, Δ17, had no impact on the predicted WLE3 secondary structure, while the smaller Δ3 deletion completely changed the conformation of the whole construct (Figure 4-4, 4-6). Δ17 essentially deletes WLE2, but the remaining nucleotides still form a stem-loop and do not appear to affect WLE3. Δ17 does influence minor changes in the base pairing of the sequences downstream of the WLE2 region, which could, in turn, modify the tertiary structure and somehow sterically hinder RNA binding proteins. It is also possible that the region directly downstream of WLE2 acts as a flexible linker that allows bending of the other stem-loops in three dimensional space. Such a region is predicted to exist in the 3' UTR of *bcd* mRNA (Brunel and Ehresmann, 2004). It is unlikely that the reason Δ17 does not localize is because of the specific bases deleted, as our results show that the larger Δ16 deletion (Figure 4-4), which is missing all the nucleotides deleted in Δ17 plus additional flanking sequence, still localizes normally. The Δ16 results further support the hypothesis that the structure of the RNA, and not just the primary sequence, plays a role in the ability of RNAs to localize. Despite the importance of structure, the predicted structure of Δ16 more closely resembles that of Δ17, than wild-type (Figure 4-4).

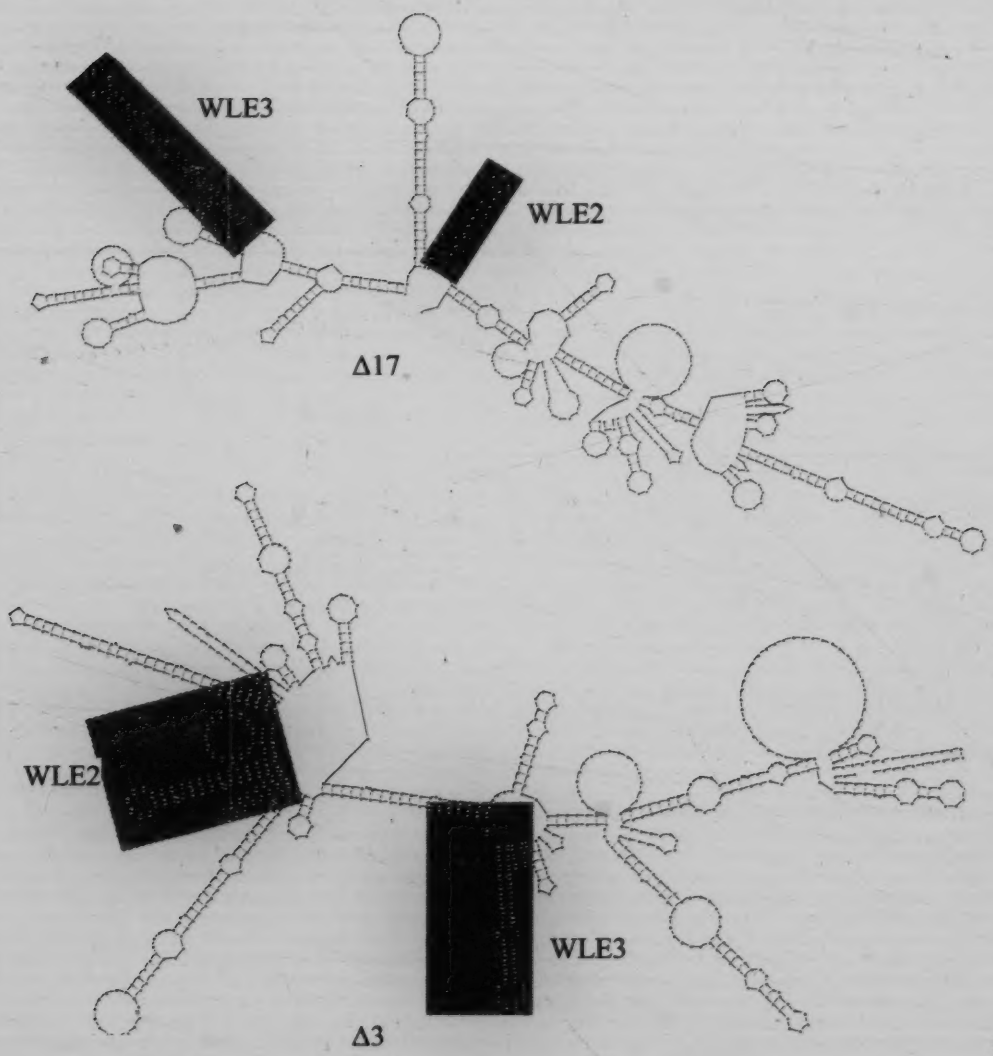

Figure 4-6: The predicted structures of the Δ17 and Δ3 mutations. Computer modelled secondary structures at 25°C of the two mutations that prevent localization of WLE2-3.

The observed effect of Δ3 on the predicted secondary structure of WLE2-3 fits better with the hypothesis that the secondary structure of WLE3 is important for its function (Figure 4-4, 4-6). It fits with the model which predicts that changes in the secondary structure of a transcript may alter its ability to localize. There are however, mutations that do not support the secondary structure – function model. Mutations such as Δ2, Δ9, Δ13, Δ15, LS1 and LS14 are also predicted to induce major conformational changes along the length of the entire WLE2-3 construct, yet they still appear to localize normally in the direct injection assay. This suggests that either our hypothesis about the importance secondary structure is wrong, or it reinforces the idea that the computer generated secondary structures are not necessarily correct, and to fully understand the nature of these structures, a more practical approach must be taken. The current algorithms used to predict the secondary structures of RNAs are good for short sequences at 37°C, but longer sequences or those folded at different temperatures are not as well calculated because the thermodynamic data used to calculate the enthalpies of these structures are done at 37°C and extrapolated to 25°C (Zuker, 2003).

WLE2 is able to form complexes with the *wg* 3' UTR

WLE2 appears to have an important role in intermolecular interactions with other RNA complexes, as co-injection with FL *wg* 3' UTR leads to the apical localization of WLE2. The WLE2-3 sequence also appears to act as a carrier for WLE2 sequence, but co-transport with this construct is not as strong, suggesting that there is something upstream of nucleotide 355, contained in the FL construct but not in the WLE2-3 construct, that augments co-transport. These results suggest that one role of WLE2 may be the formation of dimers or multimers. Our interpretation of the data does not distinguish whether multimerization takes place at a RNA-RNA level, or in large RNP complexes. Our anti-sense positive control data show that RNA-RNA based interactions are sufficient to drive the localization of an otherwise unlocalized transcript. In addition, formation of intermolecular RNA dimers has been found to be important in the transport of RNAs such as *bcd* (Ferrandon et al., 1997; Snee et al., 2005), *osk* (Hachet and Ephrussi, 2004) and *hairy* (Bullock et al., 2003), therefore it would not be too surprising if the *wg* 3' UTR also has this ability. We have not excluded the possibility that these

interactions are being mediated by intermediate proteins such as *staufen* which is known to have multiple RNA binding sites and is believed to participate in RNA localization (Ramos et al., 2000).

Computer aided predictions of the RNA-RNA interaction sites in the *wg* UTR have not been successful in identifying a specific region involved in this phenomenon. Bi-molecular folding of WLE2 and FL UTR lead to some unusual base paring at the 5' and 3' end of both strands, and a general unfolding of the secondary structures, but these unusual formations can be attributed to the algorithms used to calculate them. In contrast, dimerization of *bcd* however, is not believed to alter the secondary structures of the dimerization domains, nor the rest of the transcript (Brunel and Ehresmann, 2004).

Formation of RNA multimers presents an interesting mechanism which a cell can use to conserve energy. Given the large numbers of localized transcripts within the *Drosophila* embryo, moving multiple messages in large RNP complexes in each trip to the embryonic periphery is more efficient than motor proteins making trips for each individual transcript. This simultaneously saves energy used in transport and reduces the number of motor proteins necessary. Since there is evidence for a common RNA transport pathway (Bullock and Ish-Horowicz, 2001; Wilkie and Davis, 2001), moving multiple, different messages is also possible. Furthermore, transcripts that do not have a transport sequence, but are able to dimerize with transcripts that do, can also be transported by hitching a ride. However, our results show that it is unlikely WLE2 is piggybacking on other apically localized RNAs, because in a wild-type embryo, all the apically localized pair-rule transcripts are endogenously expressed at the time WLE2 is injected. If WLE2 was piggy backing on these pair-rule transcripts, it would be expected to localize normally, yet it appears only to localize when injected with sequences derived from the *wg* 3' UTR. Since motor protein-mediated transport of *wg* and other pair-rule transcripts happens rapidly within cells, and since the WLE2 sequence is injected quite far away from the nuclei, it is possible that the injected RNA never comes into contact with the pair-rule RNA that is exported from the nucleus and quickly transported to the apical cortex. To investigate this possibility, WLE2 should be co-injected with *in vitro* transcribed pair-rule RNA. If apical localization of WLE2 does not take place, the results will strengthen our conclusion that WLE2 does not multimerize with pair-rule transcripts.

It has not been ruled out that the localization mediated by WLE3 or any other sequence in the *wg* UTR is not due to dimerization with another apically localized RNA. Even the FISH results, which show localization at a time when pair-rule transcripts are no longer expressed can not rule out the existence of other, as yet unidentified, apically localized RNAs that are co-transporting *wg* transcripts. However, ruling out the possibility of "passive" transport by dimerization would be very difficult, as it requires the isolated expression of *wg* in an embryo, a process that would be lethal.

The differences observed in the ability of the FL 3` UTR construct and the WLE2-3 construct used to transport WLE2 can arise from a number of factors. WLE2 could be interacting with the WLE1, or with other regions within the 3' UTR. Perhaps this interaction takes place near the 355 nucleotide boundary where the WLE2-3 construct begins. FL sequence would therefore have the sequences flanking this area, whereas WLE2-3 would only have sequences downstream of 355. As a result, only part of the WLE2 sequence may bind the partial region present in the WLE2-3 construct, or the folding of the region might be affected such that WLE2 interaction is reduced. Another possibility is that WLE2 is able to dimerize with multiple, semi-redundant, co-operative regions of the FL 3' UTR. If one or more of these regions lie before nucleotide 355 and one or more after, then FL UTR would be expected to bind WLE2 more strongly than WLE2-3.

The negative controls rule out the possibility that these RNA-RNA interactions are mediated by the many large fluorophores incorporated into the sequence. If these were responsible for the intermolecular bonding that was observed, then we would have expected a similar, non-specific interaction to take place with the LacZ negative control RNA, however, our results show that this does not occur. This can be further tested by co-injecting labelled WLE2 RNA with unlabelled FL transcripts. With this combination one would be unable to track the transport of the injected FL transcripts, but it would be assumed that the FL sequence localizes normally. Because the FL sequence is not labelled with any fluorophores, any apical transport of WLE2 could be attributed to specific interactions with the FL sequence, and not interactions between fluorophores.

It is possible that the co-transport observed was mediated by base pairing between the two injected sequences, and that perhaps this does not normally take place *in vivo*.

The positive control in which anti-sense WLE2 RNA was co-injected with FL sequence demonstrated that base pairing is sufficient to direct the co-transport of a sequence that would otherwise have no ability to localize. We observed strong co-transport of sequences having as little as 30 nucleotides anti-sense to FL UTR (data not shown). Complementary pairing of 30 nucleotides is unlikely the minimal number necessary for co-transport, but that is the smallest stretch we tested.

The validity of the direct injection assay

The majority of our constructs were tested only by direct injection. The injection of RNA labelled with fluorescent nucleotide conjugates has been widely used as a quick method of assessing motor protein mediated transport of various RNAs. The first example of this was the injection of fluorescently labelled MBP into oligodendrocytes (Ainger et al., 1993). Later, this technique was adopted by fly biologists to study RNA transport in oocytes and embryos (Glotzer et al., 1997; Lall et al., 1999). Although this technique has been widely used in *Drosophila* and other species, seldom has there been an extensive study done to compare the results from this assay to that of FISH

A number of drawbacks may confound the results obtained from the direct injection assay. 1) Direct injection does not exactly mimic *in vivo* conditions, since *in vitro* transcription of the injected RNA is done in the absence of nuclear and cytoplasmic factors that may be required to help the RNA form higher order secondary and tertiary structures, and have been shown to be important in the localization of other transcripts (Hachet and Ephrussi, 2004). 2) The addition of sterically bulky fluorescent conjugates may hinder recognition of the RNA by the transport machinery or may influence the folding of the RNA such that it is no longer recognized. 3) The RNA is exposed to high pressures during injection, which may lead to the formation of otherwise thermodynamically unfavourable structures. 4) The concentrations at which the RNA is injected are not normally observed *in vivo*, and injections of lower RNA concentrations limits our ability to follow the RNA in real-time due to limitations in the sensitivity of microscopy equipment, and the short half-lives of some of the RNAs injected. 5) The syncytial blastoderm stage lasts only for the first 3 hours of embryonic development and injections must take place during this time. This introduces problems with genes that are

not normally expressed during this stage of development. *wg* happens to be a gene that is normally expressed after cellularization. 6) The gradual disappearance of the injected RNA does not necessarily indicate a non-localizable sequence, because, at least on our microscope set-up, the limited penetration of confocal lasers does not allow visualization of signal more than three quarters of the depth of the embryo away from the objective. Since the RNA will be transported to the nearest apical surface, if it is injected above the center of the embryo, it will be transported away from the objective. This will appear as though the RNA is diffusing and not being transported, but in fact the RNA is being transported away from the objective. Because of this, a negative result must be tested repeatedly, whereas three trials for a positive result is usually sufficient to conclude whether it has localization ability. 7) Transport of the RNA away from the microscope objective also means that the results for the direct injection assay are not quantifiable, because one can never be certain of the amount of injected RNA present in a particular plane, nor can one account for the total fluorescent RNA present in the entire embryo. Thus percentages of localized versus unlocalized transcripts are inaccurate and unreliable. Despite these factors, direct injection of fluorescently labelled transcripts appears to work for the majority of localized transcripts.

On the other hand, FISH circumvents most of these problems by necessarily forcing *in vivo* expression of the sequence being studied, but it too has some drawbacks. 1) *in vivo* expression of the sequence of interest requires sub-cloning of the sequences into a P-element vector which is then used create transgenic flies. This is a laborious, time consuming and expensive process which yields hundreds of transgenic flies that have to be maintained in lab stocks. 2) The data obtained from FISH can be difficult to analyze. For pair-rule and other genes expressed early in embryonic development, the results of FISH are unambiguous and easy to interpret due to the large, elongated, monolayer of syncytial nuclei in the embryonic periphery. However, with genes expressed after cellularization, the array of nuclei loses its regularity and smaller, more rounded cells begin to form. Without a clearly separated apical and basal cell membrane, it becomes increasingly difficult to categorize RNAs as localized or not.

Due to the relative ease of the direct injection assay, it would be preferable to use it over FISH, but due to its *in vitro* nature, it is important to validate its use as a viable

alternative to FISH. Table 4-1 is a comparison of the linker scanner mutations tested in both the direct injection assay and FISH. A computer based analysis was used to objectively categorize the FISH data. Each LS mutation was analyzed by choosing a single confocal slice containing a cross-section of adjacent nuclei expressing endogenous *wg* and the UAS>lacZ-WLE2 fusion transgene under the control of an *en*-Gal4 transcriptional activator. These nuclei were divided into three equally sized portions consisting of apical, middle and basal regions. ImageJ and Excel were used to calculate an integrated density value representing the proportion of RNA in each region as a function of the total RNA present. Averages of a minimum of 4 different embryos were used to calculate the average proportion of RNA in the apical region. If greater than 45% of the total RNA was in the apical region, that construct was considered to be localized, while an apical proportion of less than 45% but greater than 40% indicated that localization was altered from wild-type sequences. Anything less than 40% was considered unlocalized, because an even RNA distribution would result in 33% of the total RNA in each of the three regions.

Table 4-1: The direct injection assay reflects the results obtained using FISH. A table comparing the localization results of the WLE2-3 construct obtained from the direct injection assay and FISH. The direct injections were sorted into three categories represented by a ** for normal localization, a * when the RNA displayed some directional transport but was unable to fully localize and a - when the RNA failed to show any directional movement. FISH results were also sorted into three categories. Single nuclei in confocal sections were divided into equal apical, middle and basal regions. An integrated density value was used as a measure of the amount of RNA present in each region as a proportion of total RNA present in that particular cell. If on average, >45% of the RNA was apical, it was categorized as **, while an apical population consisting of <45% but >40% of total RNA was categorized as * and a <40% apical RNA distribution is indicated by -.

Construct	Direct Injection	FISH
FL	**	**
WLE2-3	**	**
WLE2	-	-
LS1	**	**
LS2	**	*
LS3	**	**
LS4	**	**
LS5	**	-
LS6	**	**
LS7	**	**
LS8	**	**
LS9	**	**
LS11	*	*
LS13	**	**
LS14	**	**
LS15	**	**
LS16	**	**
Δ4	**	**
Δ6	**	**
Δ11	**	**
Δ15	**	**

Using this classification system, the FISH results closely resembled those obtained from direct injection. Even the LS11 injection that showed a partial disruption of RNA transport was considered to have altered localization ability in FISH analysis. Some results, such as those of LS2 and LS5 differ between the two assays. FISH suggests that LS2 only partially localizes and that there is a nearly uniform distribution of LS5 RNA while the direct injection results suggest that both RNA sequences localize normally. This could be due to the extremely high expression of LS5 in the transgenic strain analyzed, which results in the appearance of many foci that are likely transport intermediates on their way to the apical region. These bright foci would be measured as being basal or middle regions, but they could in fact be transported intermediates fixed before they were able to reach the apical cortex. On the other hand, the low expression of LS2 could also produce unrepresentative results, as a few semi-bright foci in the apical region could be offset by the presence of one bright focus at the nascent site of transcription in the nucleus. A simple solution to these problems would be to analyze other transformants with different expression levels of the transgene, but this would still not circumvent the other problems associated with FISH.

Direct injection provides the benefit of real-time visualization, the ability to obtain results within one day of conceiving an idea, the ability to test many transcripts in a single day and the ability to do co-injections. In comparison, FISH lacks these benefits, as it requires the cloning of the sequences to be tested into P-element transfection vectors and the creation of new transgenic flies for every construct that is to be tested. Furthermore, *in situ* hybridization is a multi-day process that requires crossing two fly strains, followed by embryo collection and fixation and the three day *in situ* protocol. It does not provide easily interpretable data and forces the use of imaging software to calculate the proportions of RNA in each region of the cell. Analysis of the data using imaging software is both time consuming and subjective despite all attempts to make it as objective as possible. The only benefit that FISH provides over direct injection is that it offers *in vivo* transcription of the RNA, which, as our results have shown in the comparison between the two assays, is not of particular importance to the localization of *wg* mRNA.

In future studies involving *wg* transcript localization, direct injection should be used as the primary method by which RNAs are tested, and some of these results, including all negative results, should be verified by FISH. Negative results could be due to very subtle changes in the conformation of the RNA that may be enhanced by the direct injection assay. The *in vivo* approach that FISH provides may help these semi-stable structures fold properly and retain their ability to localize. Differences between the two approaches could also expose these subtle conformational changes.

Future work

It is therefore important verify the conclusions on WLE2 complex formation by performing FISH. The most practical way to do this would be to create flies expressing both *en*-Gal4 and *wg*-Gal4 transgenes. This would allow the expression of WLE2 tagged with a lacZ reporter in cells that are directly adjacent to one another. If in fact WLE2 is forming a complex, it would be expected to be localized only in cells expressing the *wg*-Gal4 transgene, because only those cells would also be expressing endogenous *wg*. The identification of WLE2 as a multimerization domain helps explain the discrepancy between the original identification of WLE2 as a localization element and the lack of activity in the direct injection assay. In the original experiments (Simmonds et al., 2001) WLE2 activity was analyzed in the presence of endogenous *wg* expression and would therefore be expected to localize in those cells. Verifying WLE2 dimerization has been attempted using the *ptc*-Gal4 driver to drive transgene expression and analyzing with FISH. Wild-type *ptc* expression is seen in both *wg* expressing and non-expressing cells, however the results of these experiments were inconclusive because the *ptc*-Gal4 expression of transgenes was very low and temporally different from that of wild-type *ptc* (data not shown). The creation of an *en*-Gal4 and *wg*-Gal4 expressing fly would be relatively easy as both of these strains have been obtained, and both have been tested to ensure high and correct expression of transgenes.

Assuming that complex formation happens at the level of RNA, it is important to map out the specific sequences important in the function of WLE2 as a multimerization element. Since a number of LS mutations and deletions already exist, and since most of these have already been transcribed and fluorescently labelled, these experiments would

be relatively easy to carry out. The wild-type sequences that are mutated and fail to co-localize with wild-type FL 3' UTR upon co-injection will be considered to be important in dimerization. Co-injection of wild-type WLE2 with deletions within the FL 3' UTR will allow the identification of regions that WLE2 binds to.

Co-injection of three sequences can also help determine the WLE2 binding site within the 3' UTR. In these experiments, short complimentary oligonucleotides can be annealed to FL sequence in a one to one molar ratio. The annealed sequence can then be incubated with WLE2 and injected into embryos. If WLE2 base-pairs with the region that the oligonucleotide was directed at, it would not be expected to co-localize with the FL sequence because the oligonucleotide was competitively inhibiting WLE2 binding. This approach offers a fast method of analysing binding sites without having to create additional LS mutations and deletions. Long RNA oligonucleotides can now be chemically synthesized at a relatively low cost and with high fidelity, making this approach economical. Furthermore, several oligos can be annealed to the FL sequence at once and if WLE2 does bind to multiple regions in the 3' UTR, this method will allow the specific "knockout" of all those sites. In addition, complimentary pairing with other sequences has the potential to change the conformation of the FL sequence, which can help identify useful structures, but simultaneously confound the results because the loss of interaction was due to a conformational change and not a competitive interaction.

Summary

The data presented here fit the model where recognition of the cis-acting RNA transport sequences is a function of primary, secondary and perhaps even higher order structures. We propose that WLE2 does not function as a cis-acting localization signal as originally thought. WLE2 may function as a potentiating factor for WLE3, but it also appears to have the ability to co-transport its own sequence when co-injected with FL *wg* 3' UTR. We propose that, like other localized RNAs, the *wg* 3' UTR contains sequences such as WLE2, that allow it to form complexes with itself. It is critical to test this theory by FISH using a fly strain able to drive the expression of the WLE2-lacZ transgene in *wg* expressing and non-expressing cells. If the transgene localizes only in the *wg* expressing

cells, then further work identifying the regions important in complex formation can proceed.

As the sequences responsible for the apical localization of *wg* transcripts are better understood, it is hoped that a general consensus sequence or structure required for transcript localization will emerge. This consensus will be important in the search for other localized transcripts and trans-factors involved in its recognition. As we further dissect the RNA localization pathways that are so important in the normal function of many genes, we hope to obtain a better understanding of the processes involved in gene regulation and function. Ultimately, our hope is that this research will extend beyond *Drosophila* and aid in the development of cures for human diseases affected by RNA localization.

Bibliography

Abramoff, M.D., Magelhaes, P.J., Ram, S.J. 2004. Image Processing with ImageJ. *Biophotonics International*. 11:36-42.

Ainger, K., D. Avossa, F. Morgan, S.J. Hill, C. Barry, E. Barbarese, and J.H. Carson. 1993. Transport and localization of exogenous myelin basic protein mRNA microinjected into oligodendrocytes. *J Cell Biol*. 123:431-41.

Baker, N.E. 1987. Molecular cloning of sequences from wingless, a segment polarity gene in Drosophila: the spatial distribution of a transcript in embryos. *Embo J*. 6:1765-1773.

Baker, N.E. 1988. Embryonic and imaginal requirements for wingless, a segment-polarity gene in Drosophila. *Dev Biol*. 125:96-108.

Banziger, C., D. Soldini, C. Schutt, P. Zipperlen, G. Hausmann, and K. Basler. 2006. Wntless, a conserved membrane protein dedicated to the secretion of Wnt proteins from signaling cells. *Cell*. 125:509-22.

Bartscherer, K., N. Pelte, D. Ingelfinger, and M. Boutros. 2006. Secretion of Wnt ligands requires Evi, a conserved transmembrane protein. *Cell*. 125:523-33.

Bejsovec, A., and A. Martinez Arias. 1991. Roles of wingless in patterning the larval epidermis of Drosophila. *Development*. 113:471-85.

Berleth, T., M. Burri, G. Thoma, D. Bopp, S. Richstein, G. Frigerio, M. Noll, and C. Nusslein-Volhard. 1988. The role of localization of bicoid RNA in organizing the anterior pattern of the Drosophila embryo. *Embo J*. 7:1749-56.

Bohl, F., C. Kruse, A. Frank, D. Ferring, and R.P. Jansen. 2000. She2p, a novel RNA-binding protein tethers ASH1 mRNA to the Myo4p myosin motor via She3p. *Embo J*. 19:5514-24.

Brunel, C., and C. Ehresmann. 2004. Secondary structure of the 3' UTR of bicoid mRNA. *Biochimie*. 86:91-104.

Bullock, S.L., and D. Ish-Horowicz. 2001. Conserved signals and machinery for RNA transport in Drosophila oogenesis and embryogenesis. *Nature*. 414:611-6.

Bullock, S.L., M. Stauber, A. Prell, J.R. Hughes, D. Ish-Horowicz, and U. Schmidt-Ott. 2004. Differential cytoplasmic mRNA localisation adjusts pair-rule transcription factor activity to cytoarchitecture in dipteran evolution. *Development*. 131:4251-61.

Bullock, S.L., D. Zicha, and D. Ish-Horowicz. 2003. The Drosophila hairy RNA localization signal modulates the kinetics of cytoplasmic mRNA transport. *Embo J*. 22:2484-94.

Cadigan, K.M., and R. Nusse. 1997. Wnt signaling: a common theme in animal development. *Genes Dev*. 11:3286-305.

Carson, J.H., K. Worboys, K. Ainger, and E. Barbarese. 1997. Translocation of myelin basic protein mRNA in oligodendrocytes requires microtubules and kinesin. *Cell Motil Cytoskeleton*. 38:318-28.

Cheung, H.K., T.L. Serano, and R.S. Cohen. 1992. Evidence for a highly selective RNA transport system and its role in establishing the dorsoventral axis of the Drosophila egg. *Development*. 114:653-61.

Clamp, M., J. Cuff, S.M. Searle, and G.J. Barton. 2004. The Jalview Java alignment editor. *Bioinformatics*. 20:426-7.

Colman, D.R., G. Kreibich, A.B. Frey, and D.D. Sabatini. 1982. Synthesis and incorporation of myelin polypeptides into CNS myelin. *J Cell Biol*. 95:598-608.

Cox, R.T., and M. Peifer. 1998. Wingless signaling: the inconvenient complexities of life. *Curr Biol*. 8:R140-4.

Dalby, B., and D.M. Glover. 1993. Discrete sequence elements control posterior pole accumulation and translational repression of maternal cyclin B RNA in Drosophila. *Embo J*. 12:1219-27.

Davis, I., C.H. Girdham, and P.H. O'Farrell. 1995. A nuclear GFP that marks nuclei in living Drosophila embryos; maternal supply overcomes a delay in the appearance of zygotic fluorescence. *Dev Biol*. 170:726-9.

Davis, I., and D. Ish-Horowicz. 1991. Apical localization of pair-rule transcripts requires 3' sequences and limits protein diffusion in the Drosophila blastoderm embryo. *Cell*. 67:927-40.

dos Santos, G. 2006. The mechanism and role of apical wingless mRNA localization in Drosophila. *In* Molecular & Medical Genetics Vol. PhD. University of Toronto, Toronto.

Drummond AJ, K.M., Heled J, Moir R, Thierer T, Ashton B, Wilson A, Stones-Havas S. 2006. Geneious v2.5.4, Available from http://www.geneious.com/.

Ferrandon, D., L. Elphick, C. Nusslein-Volhard, and D. St Johnston. 1994. Staufen protein associates with the 3'UTR of bicoid mRNA to form particles that move in a microtubule-dependent manner. *Cell*. 79:1221-32.

Ferrandon, D., I. Koch, E. Westhof, and C. Nusslein-Volhard. 1997. RNA-RNA interaction is required for the formation of specific bicoid mRNA 3' UTR-STAUFEN ribonucleoprotein particles. *Embo J*. 16:1751-8.

Fjose, A., W.J. McGinnis, and W.J. Gehring. 1985. Isolation of a homoeo box-containing gene from the engrailed region of Drosophila and the spatial distribution of its transcripts. *Nature*. 313:284-9.

Gautreau, D., C.A. Cote, and K.L. Mowry. 1997. Two copies of a subelement from the Vg1 RNA localization sequence are sufficient to direct vegetal localization in Xenopus oocytes. *Development*. 124:5013-20.

Gavis, E.R., and R. Lehmann. 1992. Localization of nanos RNA controls embryonic polarity. *Cell*. 71:301-13.

Glotzer, J.B., R. Saffrich, M. Glotzer, and A. Ephrussi. 1997. Cytoplasmic flows localize injected oskar RNA in Drosophila oocytes. *Curr Biol*. 7:326-37.

Gonzalez, F., L. Swales, A. Bejsovec, H. Skaer, and A. Martinez Arias. 1991. Secretion and movement of wingless protein in the epidermis of the Drosophila embryo. *Mech Dev*. 35:43-54.

Hachet, O., and A. Ephrussi. 2004. Splicing of oskar RNA in the nucleus is coupled to its cytoplasmic localization. *Nature*. 428:959-63.

Hill, M.A., and P. Gunning. 1993. Beta and gamma actin mRNAs are differentially located within myoblasts. *J Cell Biol*. 122:825-32.

Hoek, K.S., G.J. Kidd, J.H. Carson, and R. Smith. 1998. hnRNP A2 selectively binds the cytoplasmic transport sequence of myelin basic protein mRNA. *Biochemistry*. 37:7021-9.

Hughes, S.C., and H.M. Krause. 1999. Single and double FISH protocols for Drosophila. *Methods Mol Biol*. 122:93-101.

Ingham, P.W. 1993. Localized hedgehog activity controls spatial limits of wingless transcription in the Drosophila embryo. *Nature*. 366:560-2.

Kadowaki, T., E. Wilder, J. Klingensmith, K. Zachary, and N. Perrimon. 1996. The segment polarity gene porcupine encodes a putative multitransmembrane protein involved in Wingless processing. *Genes Dev*. 10:3116-28.

Kim-Ha, J., P.J. Webster, J.L. Smith, and P.M. Macdonald. 1993. Multiple RNA regulatory elements mediate distinct steps in localization of oskar mRNA. *Development*. 119:169-78.

Kislauskis, E.H., X. Zhu, and R.H. Singer. 1994. Sequences responsible for intracellular localization of beta-actin messenger RNA also affect cell phenotype. *J Cell Biol*. 127:441-51.

Kislauskis, E.H., X. Zhu, and R.H. Singer. 1997. beta-Actin messenger RNA localization and protein synthesis augment cell motility. *J Cell Biol*. 136:1263-70.

Kloc, M., and L.D. Etkin. 2005. RNA localization mechanisms in oocytes. *J Cell Sci*. 118:269-82.

Kornberg, T., I. Siden, P. O'Farrell, and M. Simon. 1985. The engrailed locus of Drosophila: in situ localization of transcripts reveals compartment-specific expression. *Cell*. 40:45-53.

Lall, S., H. Francis-Lang, A. Flament, A. Norvell, T. Schupbach, and D. Ish-Horowicz. 1999. Squid hnRNP protein promotes apical cytoplasmic transport and localization of Drosophila pair-rule transcripts. *Cell*. 98:171-80.

Lantz, V., and P. Schedl. 1994. Multiple cis-acting targeting sequences are required for orb mRNA localization during Drosophila oogenesis. *Mol Cell Biol.* 14:2235-42.

Lawrence, J.B., and R.H. Singer. 1986. Intracellular localization of messenger RNAs for cytoskeletal proteins. *Cell.* 45:407-15.

Lipshitz, H.D., and C.A. Smibert. 2000. Mechanisms of RNA localization and translational regulation. *Curr Opin Genet Dev.* 10:476-88.

Long, R.M., R.H. Singer, X. Meng, I. Gonzalez, K. Nasmyth, and R.P. Jansen. 1997. Mating type switching in yeast controlled by asymmetric localization of ASH1 mRNA. *Science.* 277:383-7.

MacDonald, P.M. 1990. bicoid mRNA localization signal: phylogenetic conservation of function and RNA secondary structure. *Development.* 110:161-71.

Macdonald, P.M., and K. Kerr. 1997. Redundant RNA recognition events in bicoid mRNA localization. *Rna.* 3:1413-20.

Macdonald, P.M., and G. Struhl. 1988. cis-acting sequences responsible for anterior localization of bicoid mRNA in Drosophila embryos. *Nature.* 336:595-8.

Mach, J.M., and R. Lehmann. 1997. An Egalitarian-BicaudalD complex is essential for oocyte specification and axis determination in Drosophila. *Genes Dev.* 11:423-35.

Martizez Arias, A., N.E. Baker, and P.W. Ingham. 1988. Role of segment polarity genes in the definition and maintenance of cell states in the Drosophila embryo. *Development.* 103:157-70.

Masek, T., V. Vopalensky, P. Suchomelova, and M. Pospisek. 2005. Denaturing RNA electrophoresis in TAE agarose gels. *Anal Biochem.* 336:46-50.

Mathews, D.H., M.D. Disney, J.L. Childs, S.J. Schroeder, M. Zuker, and D.H. Turner. 2004. Incorporating chemical modification constraints into a dynamic programming algorithm for prediction of RNA secondary structure. *Proc Natl Acad Sci U S A.* 101:7287-92.

Matzura, O., and A. Wennborg. 1996. RNAdraw: an integrated program for RNA secondary structure calculation and analysis under 32-bit Microsoft Windows. *Comput Appl Biosci.* 12:247-9.

Molven, A., P.R. Njolstad, and A. Fjose. 1991. Genomic structure and restricted neural expression of the zebrafish wnt-1 (int-1) gene. *Embo J.* 10:799-807.

Navarro, C., H. Puthalakath, J.M. Adams, A. Strasser, and R. Lehmann. 2004. Egalitarian binds dynein light chain to establish oocyte polarity and maintain oocyte fate. *Nat Cell Biol.* 6:427-35.

Nelson, M.R., A.M. Leidal, and C.A. Smibert. 2004. Drosophila Cup is an eIF4E-binding protein that functions in Smaug-mediated translational repression. *Embo J.* 23:150-9.

Noordermeer, J., F. Meijlink, P. Verrijzer, F. Rijsewijk, and O. Destree. 1989. Isolation of the Xenopus homolog of int-1/wingless and expression during neurula stages of early development. *Nucleic Acids Res.* 17:11-8.

Nusslein-Volhard, C., and E. Wieschaus. 1980. Mutations affecting segment number and polarity in Drosophila. *Nature.* 287:795-801.

Ramos, A., S. Grunert, J. Adams, D.R. Micklem, M.R. Proctor, S. Freund, M. Bycroft, D. St Johnston, and G. Varani. 2000. RNA recognition by a Staufen double-stranded RNA-binding domain. *Embo J.* 19:997-1009.

Rijsewijk, F., M. Schuermann, E. Wagenaar, P. Parren, D. Weigel, and R. Nusse. 1987. The Drosophila homolog of the mouse mammary oncogene int-1 is identical to the segment polarity gene wingless. *Cell.* 50:649-57.

Ross, A.F., Y. Oleynikov, E.H. Kislauskis, K.L. Taneja, and R.H. Singer. 1997. Characterization of a beta-actin mRNA zipcode-binding protein. *Mol Cell Biol.* 17:2158-65.

Rubin, G.M., and A.C. Spradling. 1982. Genetic transformation of Drosophila with transposable element vectors. *Science.* 218:348-53.

Schneider, M.D., N. Najand, S. Chaker, J.M. Pare, J. Haskins, S.C. Hughes, T.C. Hobman, J. Locke, and A.J. Simmonds. 2006. Gawky is a component of cytoplasmic mRNA processing bodies required for early Drosophila development. *J Cell Biol.* 174:349-58.

Schnorrer, F., K. Bohmann, and C. Nusslein-Volhard. 2000. The molecular motor dynein is involved in targeting swallow and bicoid RNA to the anterior pole of Drosophila oocytes. *Nat Cell Biol.* 2:185-90.

Serano, T.L., and R.S. Cohen. 1995. A small predicted stem-loop structure mediates oocyte localization of Drosophila K10 mRNA. *Development.* 121:3809-18.

Shapiro, L., H.H. McAdams, and R. Losick. 2002. Generating and exploiting polarity in bacteria. *Science.* 298:1942-6.

Sharma, R.P. 1973. Wingless: A new mutant in Drosophila Melanogaster. *Drosophila Information Service.* 50.

Sharma, R.P., and V.L. Chopra. 1976. Effect of the Wingless (wg1) mutation on wing and haltere development in Drosophila melanogaster. *Dev Biol.* 48:461-5.

Simmonds, A.J., G. dosSantos, I. Livne-Bar, and H.M. Krause. 2001. Apical localization of wingless transcripts is required for wingless signaling. *Cell.* 105:197-207.

Snee, M.J., E.A. Arn, S.L. Bullock, and P.M. Macdonald. 2005. Recognition of the bcd mRNA localization signal in Drosophila embryos and ovaries. *Mol Cell Biol.* 25:1501-10.

St Johnston, D. 2005. Moving messages: the intracellular localization of mRNAs. *Nat Rev Mol Cell Biol.* 6:363-75.

Strutt, D. 2003. Frizzled signalling and cell polarisation in Drosophila and vertebrates. *Development.* 130:4501-13.

Sulston, J.E., E. Schierenberg, J.G. White, and J.N. Thomson. 1983. The embryonic cell lineage of the nematode Caenorhabditis elegans. *Dev Biol.* 100:64-119.

Surdej, P., and M. Jacobs-Lorena. 1998. Developmental regulation of bicoid mRNA stability is mediated by the first 43 nucleotides of the 3' untranslated region. *Mol Cell Biol.* 18:2892-900.

Takizawa, P.A., A. Sil, J.R. Swedlow, I. Herskowitz, and R.D. Vale. 1997. Actin-dependent localization of an RNA encoding a cell-fate determinant in yeast. *Nature.* 389:90-3.

Tanaka, K., Y. Kitagawa, and T. Kadowaki. 2002. Drosophila segment polarity gene product porcupine stimulates the posttranslational N-glycosylation of wingless in the endoplasmic reticulum. *J Biol Chem.* 277:12816-23.

Thompson, J.D., T.J. Gibson, F. Plewniak, F. Jeanmougin, and D.G. Higgins. 1997. The CLUSTAL_X windows interface: flexible strategies for multiple sequence alignment aided by quality analysis tools. *Nucleic Acids Res.* 25:4876-82.

Trapp, B.D., T. Moench, M. Pulley, E. Barbosa, G. Tennekoon, and J. Griffin. 1987. Spatial segregation of mRNA encoding myelin-specific proteins. *Proc Natl Acad Sci U S A.* 84:7773-7.

van Ooyen, A., V. Kwee, and R. Nusse. 1985. The nucleotide sequence of the human int-1 mammary oncogene; evolutionary conservation of coding and non-coding sequences. *Embo J.* 4:2905-9.

Wagner, C., C. Ehresmann, B. Ehresmann, and C. Brunel. 2004. Mechanism of dimerization of bicoid mRNA: initiation and stabilization. *J Biol Chem.* 279:4560-9.

Wagner, C., I. Palacios, L. Jaeger, D. St Johnston, B. Ehresmann, C. Ehresmann, and C. Brunel. 2001. Dimerization of the 3'UTR of bicoid mRNA involves a two-step mechanism. *J Mol Biol.* 313:511-24.

Wang, C., and R. Lehmann. 1991. Nanos is the localized posterior determinant in Drosophila. *Cell.* 66:637-47.

Warner, J.R., P.M. Knopf, and A. Rich. 1963. A multiple ribosomal structure in protein synthesis. *Proc Natl Acad Sci U S A.* 49:122-9.

Wharton, R.P., and G. Struhl. 1991. RNA regulatory elements mediate control of Drosophila body pattern by the posterior morphogen nanos. *Cell.* 67:955-67.

Wilkie, G.S., and I. Davis. 2001. Drosophila wingless and pair-rule transcripts localize apically by dynein-mediated transport of RNA particles. *Cell.* 105:209-19.

Wodarz, A., and R. Nusse. 1998. Mechanisms of Wnt signaling in development. *Annu Rev Cell Dev Biol.* 14:59-88.

Zuker, M. 2003. Mfold web server for nucleic acid folding and hybridization prediction. *Nucleic Acids Res.* 31:3406-15.